RI 8976

Bureau of Mines Report of Investigations/1985

Structural Design Considerations for Deep Mine Shafts

Analysis of Circular, Rectangular, and Elliptical Openings

By S. S. M. Chan and M. J. Beus

UNITED STATES DEPARTMENT OF THE INTERIOR

Report of Investigations 8976

Structural Design Considerations for Deep Mine Shafts

Analysis of Circular, Rectangular, and Elliptical Openings

By S. S. M. Chan and M. J. Beus

UNITED STATES DEPARTMENT OF THE INTERIOR
Donald Paul Hodel, Secretary

BUREAU OF MINES
Robert C. Horton, Director

Library of Congress Cataloging in Publication Data:

Chan, Samuel S. M

Structural design considerations for deep mine shafts.

(Report of investigations ; 8976)

Bibliography: p. 35-37.

Includes index.

Supt. of Docs. no.: I 28.23: 8976.

1. Mine shafts–Mathematical models. 2. Finite element method. I. Beus, Michael J. II. Title. III. Series: Report of investigations (United States. Bureau of Mines) ; 8976.

TN23.U43 [TN283] 622s [622'.25] 85-600073

CONTENTS

ILLUSTRATIONS

ILLUSTRATIONS--Continued

TABLES

UNIT OF MEASURE ABBREVIATIONS USED IN THIS REPORT

ft	foot	pct	percent
h	hour	psi	pound per square inch
in	inch	yr	year
in/h	inch per hour		

STRUCTURAL DESIGN CONSIDERATIONS FOR DEEP MINE SHAFTS

Analysis of Circular, Rectangular, and Elliptical Openings

By S. S. M. Chan[1] and M. J. Beus[2]

ABSTRACT

The Bureau of Mines has investigated the structural aspects of shafts and support systems using the finite-element technique. In situ field measurements in deep, vein-type metal mines show that rock stresses are often higher in the horizontal direction than the vertical, and unequal in the horizontal plane. These data and laboratory and field-determined physical properties were used as input to analytical studies.

Various design and construction parameters were investigated to determine the effect on shaft stability. Rectangular shafts were studied in detail to determine the effects of applied stress ratio, shaft orientation and dimension, influence of interbedded quartzite and argillite, and rock fracturing. Various support systems were analyzed, including concrete lining, timber, and steel sets. Circular configurations were investigated to evaluate yield zones and liner thickness. Elliptical shafts and time effects were briefly evaluated to illustrate shape and time effects and demonstrate the methodology.

It is shown that the magnitude, direction, and ratio of applied stress and rock mass anisotropy are keys to determining shaft stability. A realistic conceptual framework was developed with which to examine the rock and support interaction in deep mine shafts. Structural analysis techniques overcome some of the historical difficulties with shaft design by defining the field data requirements and structural sensitivity of various design and construction parameters.

[1]Mining engineer, Spokane Research Center, Bureau of Mines, Spokane, WA; professor of mining engineering, University of Idaho, Moscow, ID.

[2]Mining engineer, Spokane Research Center, Bureau of Mines, Spokane, WA.

INTRODUCTION

In recent years a need has developed for mine shafts of more sophisticated design both in established mining areas and in newer mining districts. The successful mining of deeper and lower grade ore bodies requires faster sinking methods, higher tonnage, lower maintenance, and better ventilation.

Traditionally, the term "shaft design" has meant specification of the hoisting capacity, ventilation requirements, skip, cage, and guide design, optimum location, hoisting plant, and sinking method (29, 41).[3] Extensive attention has always been paid to the shaft construction technique and service requirements. Considerable inertia against trying new techniques in a given area is evident, even though these techniques may have been successful and economical elsewhere. Considering the importance and capital expenditure requirements of deep mine shafts, a high degree of confidence must be developed in new design approaches before their use can be justified.

The basic structural considerations in shaft design are configuration and ground support. The two most common shapes are circular and rectangular. A typical rectangular shaft section is shown in figure 1*A*. Ground support systems include concrete, timber sets, steel sets, rock bolts, and steel liners. Figure 1*B* shows the timber support and compartment layout at a typical rectangular shaft station.

The inherent advantages and/or disadvantages of various shaft designs are well known. Circular concrete-lined shafts have minimal resistance to ventilation airflow, are virtually fireproof, and are best able to resist uniform external loads. However, concrete does not yield significantly, and potential failure conditions cannot be easily detected or repaired. Therefore, timber-supported, rectangular shafts predominate in many older and deeper mining districts with highly stressed, heavy ground because the sets can be relieved and reblocked when squeezed out of alignment. However, the constant maintenance and repair requirements result in exposure to inherently dangerous working environments and excessive operating costs.

A dilemma exists in many older mining districts--circular, concrete-lined openings have many desirable features, provided they are strong enough to withstand the stresses and displacements involved. Rectangular, timber-supported shafts have proved adequate over the years, especially in deep vein-type mines. Therefore, when new shafts are to be sunk, or existing shafts deepened, the tendency has been to use configurations that have proved successful in the past.

McWilliams (35), in his study of the Coeur d'Alene mining district in Idaho, stated "...shafts are designed with the compartments alined side by side, and with the long horizontal axis oriented normal to the bedding of the country rock. Experience has shown that such a position is best able to resist rock pressure encountered at depth." However, the implication of increased maintenance and repair requirements on ever-deepening shafts is becoming a more important consideration.

The Bureau has initiated several projects to advance the state-of-the-art of shaft design, particularly in deep, vein-type metal mines. The primary objectives are to (1) define the nature, magnitude, and direction of the stresses acting around shaft openings, (2) determine the structural sensitivity of various shaft designs to changes in applied load, shape, orientation, and support, (3) conduct prototype laboratory and full-scale field studies, and (4) establish design criteria. The Coeur d'Alene mining district in northern Idaho is an ideal test area because of the availability of test sites and because it is typical of a deep-vein mining area experiencing shaft stability problems.

Several stages of investigation are being conducted including (1) small-scale field and laboratory studies to determine in situ stress, physical properties, and stress and displacement distribution in

[3]Underlined numbers in parentheses refer to items in the bibliography at the end of this report.

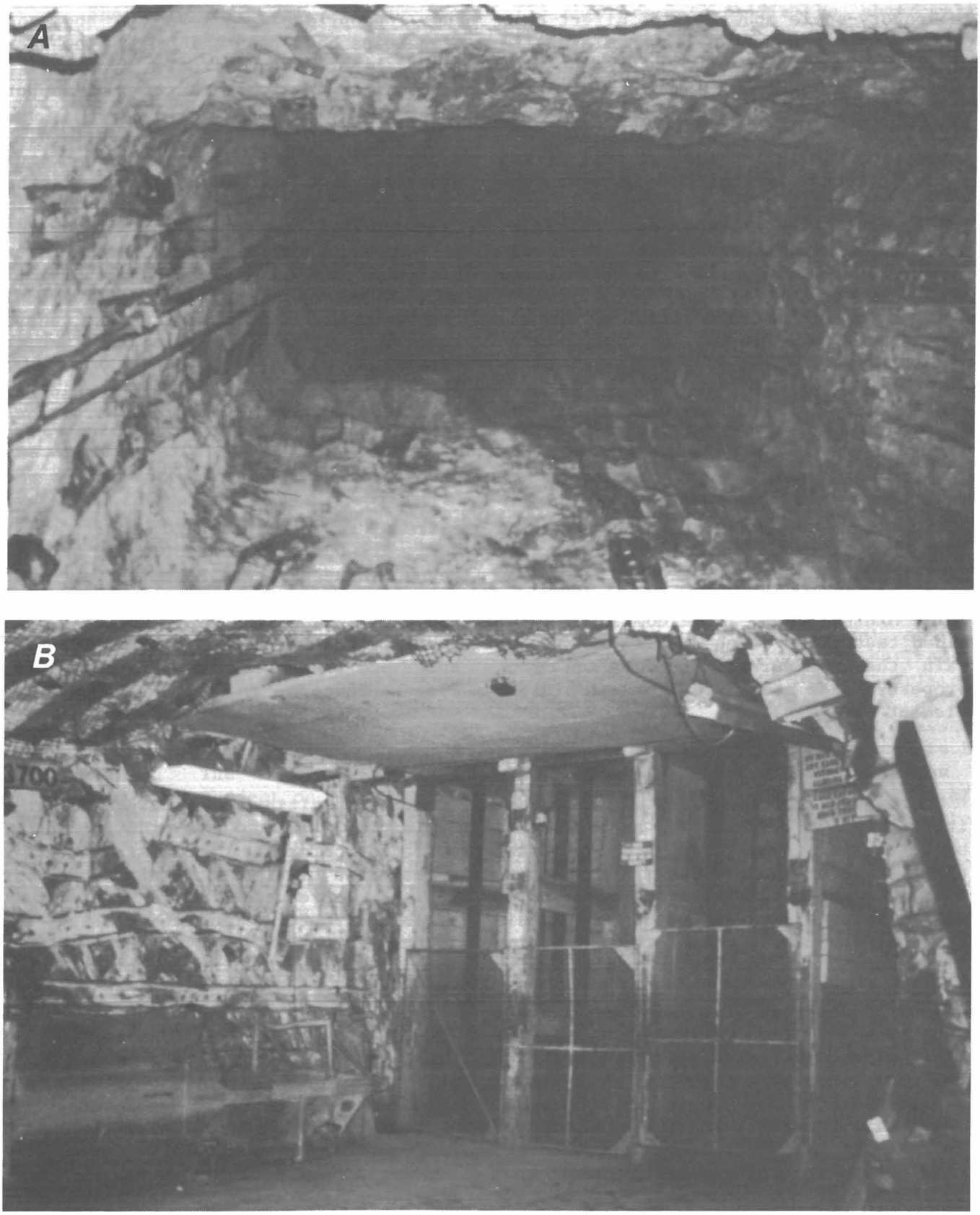

FIGURE 1. - Typical rectangular shaft and station in deep vein-type mine. *A*, Rectangular shaft section; *B*, timber support and compartment layout.

laboratory-scale models, (2) direct comparison of circular and rectangular half-scale test shafts, (3) instrumentation and analysis of full-size shafts, and (4) extensive two- and three-dimensional finite-element and boundary-element analysis to establish design guidelines and compare actual versus theoretical behavior. Results of small-scale in situ and laboratory stress and physical property measurements have been published (3). Construction of the test shafts is also complete.

This report presents results of two-dimensional, elastic, plastic, and visco-elastic, finite-element analyses. Emphasis is on rectangular shafts, as this is where analysis is lacking. Input data are based on actual in situ measurements, and appropriate load ranges and rock properties have been selected. The background literature currently available on structural design of shafts and support systems is also examined to put the current analyses into proper perspective.

Application of the finite-element technique for simulation of horizontal cross sections of deep, vertical mine shafts is illustrated. Aside from the "fixed" conditions of in situ stress, rock properties, and geologic conditions, the "variable" design parameters are considered in the analysis. This includes size, shape, and orientation of the opening and the type and dimension of support. The results can be used either as a guide for detailed shaft design analysis or to establish design criteria.

ACKNOWLEDGMENTS

The authors appreciate the cooperation given by various Coeur d'Alene mining district operators, including Callahan Mining Corp., Hecla Mining Co., and Sunshine Mining Co. These companies provided test sites which enabled us to obtain the considerable stress and rock property data needed to conduct finite-element analysis.

Credit is also given to Doug Tesarik, Bill Vilwock, and Gene Stone of the Bureau of Mines Spokane Research Center for their computer assistance. Agbabian Associates of El Segundo, CA, are also acknowledged for their technical assistance and interpretation of the finite-element codes.

BACKGROUND

The design of underground mining openings and support systems is based largely on past experience. Design details are often transferred from one mining property to another with similar ground and/or mining methods and adapted to the conditions of that particular mine. As time progresses, the designs are modified by trial and error.

Mining openings often suffer from a lack of detailed structural design. Civil structures such as transportation and water supply tunnels and underground power stations are designed to protect the public interest, and the penalties of poor design are severe. Consequently, this design technology has advanced at a rapid rate.

Somewhat in contrast, mine openings generally have more complex and varied stress and geologic conditions due to the mineral deposition environment and mining activities. In addition, they do not require the permanence and aesthetic attributes of a civil structure. Prior mine design research also has focused primarily on horizontally oriented openings such as tunnels, drifts, and underground chambers. A frequent misconception is that the same design approach can be used for mine shafts. Furthermore, to the authors' knowledge, detailed instrumentation and analysis in shafts in the United States has been attempted only once, in a concrete-lined shaft in sedimentary formations (1, 48). Structural information on deep shaft design is, therefore, scarce, and a definite need exists for additional in situ data and shaft and support system analysis to establish design criteria.

SHAFT LOADS AND THE IN SITU STRESS FIELD

The orientation, magnitude, and nature of the stresses around an underground opening consist of "induced" components, or those due to excavation, superimposed on the "natural" components; that is, residual, tectonic, and gravitational loads. Gravity and tectonic forces, both horizontal and vertical, are normally in a state of equilibrium prior to mining or tunnel construction. Extraction of some of the rock in this mass disturbs the equilibrium by removing the balancing forces and induces stresses in the form of redistribution and concentration. The load that was carried by the removed rock is transferred to the rock adjacent to the opening. As the face is advanced, its supporting effect is lost, and this additional stress is also carried by the remaining rock (47). Additional loading beyond the yield point might occur as a result of plastic and creep characteristics of the remaining rock mass, aging of concrete in support structures, and effect of temperature and humidity changes on the exposed rock and support system.

According to Terzhagi's well-known theory (45), rock responds to this change in load by deforming, resulting in a lowering of the roof and deflection of the tunnel walls. The magnitude of such deformation is dependent on the capability of the rock to resist deformation and the amount of load change. An area of deformed rock exists around an underground opening, the extent dependent upon the type of ground, the construction technique, and the size and depth of the tunnel.

The same rock load theories developed by Terzhagi for use in tunnels are often considered valid for shafts (55). Obviously, the in situ stress field and inherent rock strength play a significant role in the design approach for shafts. However, the concept of providing support for a gravity-loaded rock mass is not valid.

Mine shafts differ structurally from mine tunnels or drifts in several ways: (1) The stress magnitude generally increases as the shaft bottom is advanced, (2) the rock material in the shaft walls behaves differently under the influence of gravity, and (3) the construction method and support concepts and resulting support-rock interaction is different. Therefore, the traditional design assumptions regarding applied loads, support interaction, and failure modes applicable to tunnels are not necessarily adaptable to shafts. In addition, the consequences of shaft failure are potentially more catastrophic than for a tunnel failure. Failed material presents a hazard at all points below, not just at an isolated point, thus magnifying the risk to equipment and personnel in the shaft.

There are two approaches concerning the source of shaft loading: that resulting from the in situ rock stress, and that from ground water. Water around a lined shaft results in a uniform pressure and is simply a hydrostatic head behind the lining equal to the height of the column of water. Rock pressure is dependent on several factors--density and homogeneity of the rock mass, physical properties, construction variables, and tectonic and residual stress. For vertical shafts, the magnitude and ratio of horizontal ground stress are often the most critical and difficult to define in terms of determining shaft stability. Rock pressure in the shaft is normally assumed to be uniform, with a magnitude based on a lithostatic condition and Poisson's effect. If the stress in the horizontal plane is not uniform owing to tectonic activity, anisotropy, and nearby mining, design of the shaft and support structure becomes considerably more complex.

Recent measurements by the Bureau have shown that in situ field stress and physical properties can be extremely variable (4). For example, the horizontal stress often exceeds vertical stress, a fact that has also been reported in about 75 pct of measurements conducted worldwide (34). Several theories support the existence of high horizontal stress components, including those by Bucky (6) and Hast (23). According to these theories, the greatest deviation of horizontal stress from that determined to be due to the weight of the overlying overburden occurs in mountainous terrain, in areas

where the near-surface crust has not been relieved by faulting and where a large amount of folding or surface erosion has occurred. This is precisely the case in the Coeur d'Alene mining district, and stress field measurements and related observations support these hypotheses (4).

Table 1 shows the principal stress ratios with respect to depth determined at various mines in the Coeur d'Alenes. The ratio of the major principal stress to the minor principal stress is as high as 3.18 at the Sunshine Mine, with a low of 1.25 at the Crescent Mine. This indicates biaxial loading conditions due to tectonic influence. Also, the stress ratio implies that biaxial load conditions might prevail at deeper mining horizons instead of plastic flow and uniform loading.

In situ stress information is further resolved for vertical and horizontal stress components (table 2), showing the ratio between horizontal and vertical stress and the biaxial horizontal stress condition, in order of increasing depth of overburden. The average ratio of maximum horizontal to vertical stress (σ_{h_1}/σ_v) is 1.54 with the ratio of maximum to minimum horizontal stress ($\sigma_{h_1}/\sigma_{h_2}$) averaging 1.66.

All of the data analyzed from 1967 to the present time show that (1) the vertical stress is comparable to what might be expected from a gravity-loaded mass, (2) the horizontal stresses are greater than the vertical, and (3) the horizontal stress ratio ranges from near 1:1 to almost 3:1 (4). Consideration of the in situ stress field in the shaft design process is obviously of prime importance, particularly at depths where the in situ stress could exceed rock strength.

TABLE 1. - Principal stress ratios in the Coeur d'Alene mining district

Mine	Overburden, ft	Principal stress ratio (σ_1/σ_3)
Caladay.....	1,220	2.65
Galena.....	4,000	1.85
Lucky Friday...	4,250	3.11
Sunshine.....	4,800	3.18
Crescent.....	5,300	1.25
Silver Summit..	5,500	2.80
Star.....	7,340	1.78

TABLE 2. - Vertical and horizontal stresses, Coeur d'Alene mining district

Test site	Overburden, ft	Vertical stress (σ_v), psi	Maximum horizontal stress (σ_{h_1}), psi	Minimum horizontal stress (σ_{h_2}), psi	σ_{h_1}/σ_v	σ_{h_1}/σ_h
Shaft station, Caladay Project.....	1,200	1,450	1,280	820	0.88	1.56
3400 level, Galena Mine.....	4,000	5,500	13,000	9,540	2.37	1.36
4250 level, Lucky Friday Mine.....	4,250	4,770	9,520	6,730	2.00	1.42
4800 level, Sunshine Mine.....	4,800	7,420	7,220	4,000	.97	1.81
3300 level, Crescent Mine.....	5,300	6,300	7,830	6,280	1.24	1.25
4000 level, Silver Summit Mine.....	5,500	7,870	14,720	5,390	1.87	2.73
7300 level, Star Mine.	7,340	7,280	10,430	6,880	1.43	1.52

Physical properties, especially the strength and elastic parameters of rocks, have also been determined at numerous mines in the district (3). Findings indicate that (1) the rocks are hard and brittle and deform elastically, (2) the strength of the rock samples is highly variable, depending upon the mineral content, fracturing, and interlayering conditions, (3) the elastic properties are variable and are easily affected by the degree of confinement, and (4) the rock masses in the district often exhibit small, steady-state creep displacements at low rates.

There are numerous geologic observations in the Coeur d'Alenes that support the measured data. For example, according to a popular hypothesis of the tectonic evolution of the Coeur d'Alene mining district (27), there were several stages in the development of the tectonic setting of the district. A strong, horizontal compressive force occurred in a general northeast-southwest direction forming a series of anticlines, synclines, and some faults with parallel axes. The regional ground force was then reoriented to a somewhat east-west direction, the Osburn fault and its branches were formed, and the existing folds and faults were offset. Finally, igneous intrusions, mineralization, and the formation of veins added to the complexity of the structural pattern. Correlation of this hypothesis with measured field data (2, 4) indicates that the in situ stress field is related to past and present regional tectonic forces, even though minor local modifications are expected from the effects of mining.

Other indications of unequal horizontal stresses and anisotropy include the observation of failure modes in 4- to 7-ft-diam, machine-bored, vertical raises. These are identified as shear failures resulting from a large difference in secondary principal stresses in a plane normal to the axis of the raise bore. Figure 2 shows typical failure patterns in a 5-ft-diam raise.

Core disking has also been encountered in numerous borehole drillings in the district. Obert states that this condition exists when the horizontal stress is numerically greater than the vertical stress in a vertical borehole (40). Or, in the case of a horizontal borehole, either a vertical or horizontal stress normal to the borehole axis is greater than the horizontal stress along the axis of the borehole.

STRESSES AROUND SHAFTS

The magnitude and distribution of stress around shafts may be determined analytically by mathematical solution or physical modeling, empirically from statistical analysis, i.e., RQD or Q studies, or in situ instrumentation and monitoring. Stresses and displacements resulting from an analytical solution are dependent on the forces applied to the model boundaries and the physical properties determined for the rock mass. The quality of the solution is dependent on the quality of the input data and the skill of the investigators in defining the structural complexities in the model.

Structural design of circular shafts consists primarily of specifying the required thickness of the lining to support a hydrostatic loading from water pressure and/or loading from rock pressure. Other design variables that may be considered are physical properties of the lining, use of backpacking, shaft size, distance from the face before permanent support is installed, and initial support, such as shotcrete bolting. Circular openings are best suited for a uniform outside-pressure distribution, resulting in a uniform stress concentration in the shaft wall and the lining. Concrete-lined circular shafts can be considered analogous to thick-walled cylinders, or a hole within an infinite elastic plate; and closed-form solutions are well developed for calculating critical stresses, lining thickness, strains, and deformations.

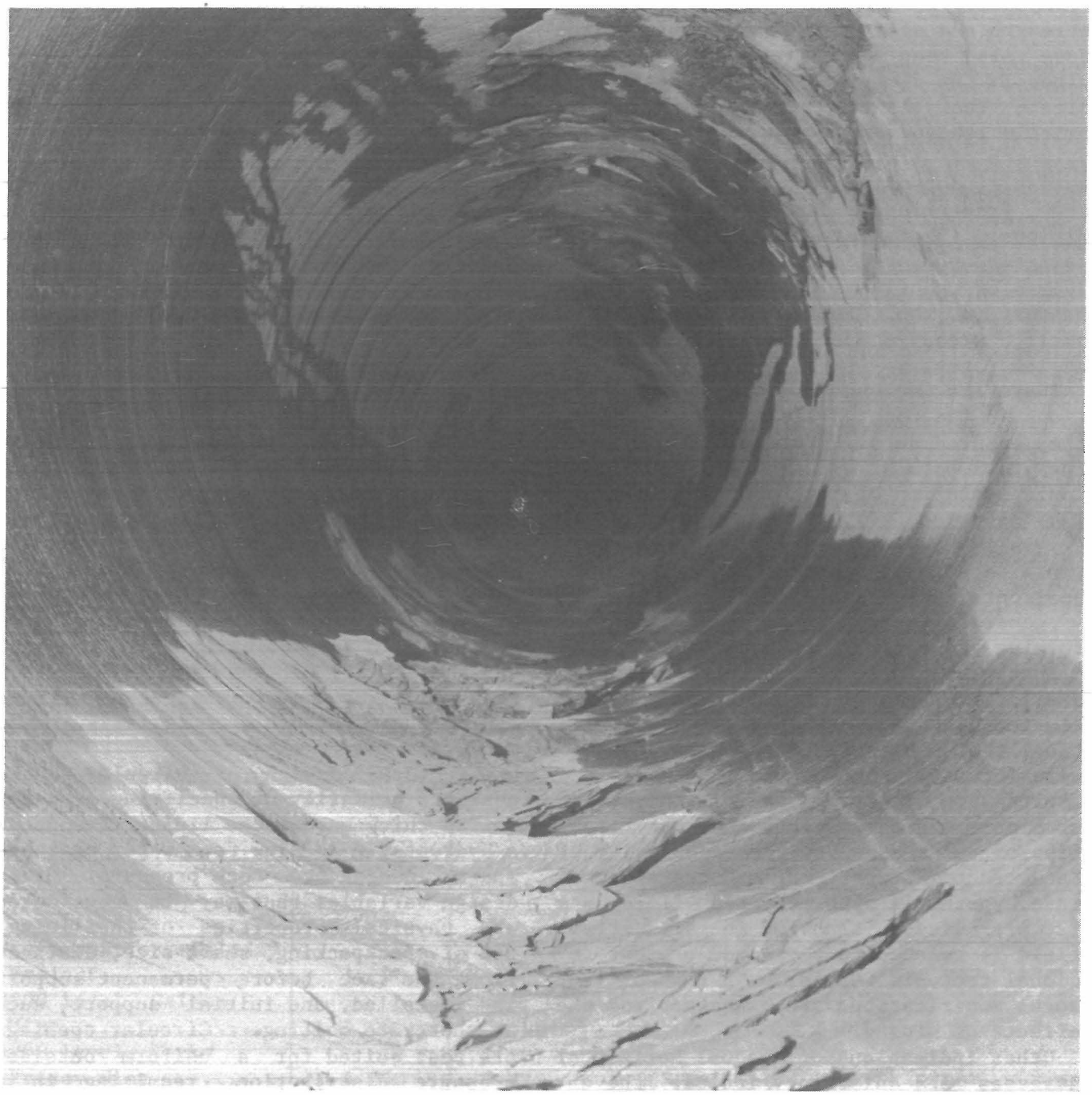

FIGURE 2. - Shear failure in 5-ft-diam raise bore.

The primary structural consideration for rectangular shafts consists of specifying orientation, with respect both to the prevailing stress field (if it is known or can be reliably inferred) and to weakness planes in the rock mass. Orientation has historically been based on minimizing the exposure of individual bedding planes, which are often considered to act as a beam or flat plate with fixed ends. Size of the shaft and ratio of the length of axes are also structurally important, although most often these are specified based on production and ventilation requirements.

Mathematical relationships to determine the stress distribution around rectangular shafts are considerably more complex than for circular shafts. The equations contain curvilinear coordinates and complex variables (50-53) and characterize the shaft corners as ellipses because of infinite stress concentrations at perfectly sharp corners. Obert and Duvall (39) determined the stress concentration pattern for rectangular shapes using photoelastic modeling techniques for different applied loads and varying ratios between stresses and major and minor axes. Their results are based on loading for horizontal openings; however, they might be considered valid for vertical shafts in a homogeneous elastic medium without support.

The calculation of the radial and tangential stresses around circular shafts, on the other hand, is well documented. If there is no evidence of tectonic loading, and if a dry shaft is desired, a hydrostatic lining is designed (29, 52). For a uniform field stress, p_o, and the outside radius equal to infinity, Lame's thick-wall cylinder equations are used (51, 53):

$$\sigma_r = p_o\left(1 - \frac{a^2}{r^2}\right), \qquad (1)$$

$$\sigma_\theta = p_o\left(1 + \frac{a^2}{r^2}\right), \qquad (2)$$

where σ_r, σ_θ = radial and tangential stresses, respectively,

a = shaft radius,

and r = radial distance from center of shaft to any point in the rock.

When the shaft is lined, the radial and tangential stresses in the lining may also be calculated from the thick-wall cylinder equations, providing the applied load (p_o) is uniform, as

$$\sigma_r = \left(\frac{b^2}{b^2-a^2}\right)\left(P_o\right)\left(1 - \frac{a^2}{r^2}\right), \qquad (3)$$

$$\sigma_\theta = \left(\frac{b^2}{b^2-a^2}\right)\left(P_o\right)\left(1 + \frac{a^2}{r^2}\right), \qquad (4)$$

where a = inside radius of the lining,

b = outside radius of the lining,

r = radial distance from center of shaft to the point of interest,

and P_o = uniform applied load on the lining.

It is obvious from the above equations that the tangential stress in the lining is at a maximum value and that the radial stress is zero at the inner surface of the lined shaft when $r = a$. Figure 3 shows a simplified cross section of a lined shaft and the normal stress notation.

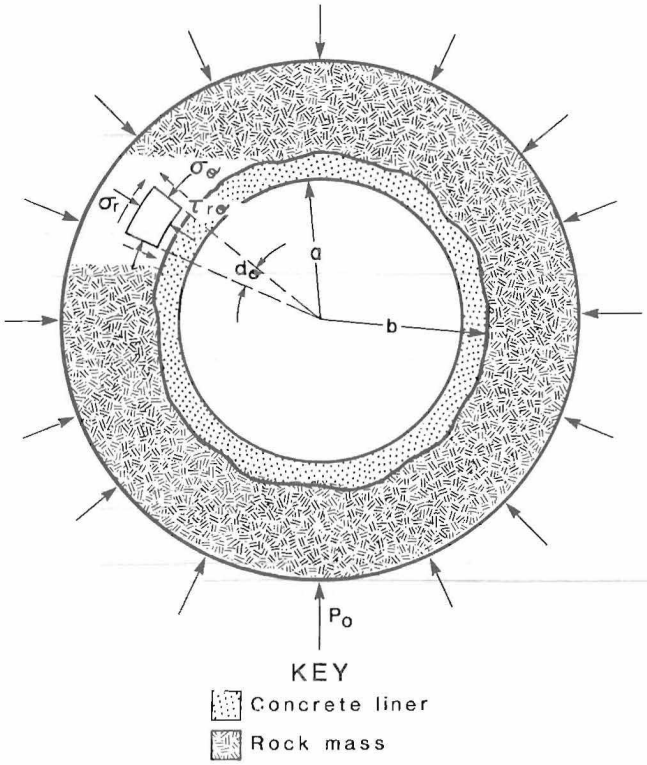

FIGURE 3. - Applied loads and internal stresses in lined circular shaft.

For unlined circular shafts in unequal stress fields, the radial, tangential, and shear stresses at any point may be calculated from the Kirsch equations (39, 53) as a hole in an infinite plate as follows:

$$\sigma_r = \left(\frac{S_x + S_y}{2}\right)\left(1 - \frac{a^2}{r^2}\right) + \left(\frac{S_x - S_y}{2}\right)\left(1 - \frac{4a^2}{r^2} + \frac{3a^4}{r^4}\right)\cos 2\theta, \quad (5)$$

$$\sigma_\theta = \left(\frac{S_x + S_y}{2}\right)\left(1 + \frac{a^2}{r^2}\right) \left(\frac{S_x - S_y}{2}\right)\left(1 - \frac{3a^4}{r^4}\right)\cos 2\theta, \quad (6)$$

and

$$\tau_{r\theta} = \left(\frac{S_y - S_x}{2}\right)\left(1 + \frac{2a^2}{r^2} - \frac{3a^4}{r^4}\right)\sin 2\theta, \quad (7)$$

where a = shaft radius,

r = radial distance from the center of the shaft to any point in the rock,

θ = polar coordinate, horizontal axis as $\theta = 0°$,

S_x and S_y = horizontally applied field stresses, 90° apart,

and $\tau_{r\theta}$ = maximum shear stress.

When a lined circular shaft is acted upon by unequal horizontal pressure, the Kirsch equations may be further developed in terms of radial or tangential stress at any region in the medium. Dar (13-14) has completed this work and programmed the equations for computer analysis. Ostrowski (41) has also presented solutions to nonuniform distribution of loads around lined circular shafts, according to the "degree of nonuniformity" of applied loads.

Equations 1 through 7 for lined and unlined vertical shafts are based on elasticity and the "maximum stress" failure criteria for single openings in competent massive rock formations. The state of stress thus computed is due entirely to elastic deformation that may occur prior to any failure condition in the rock surrounding the shaft. If the zone of rock around the shaft has failed, the appropriate equations are those governing plastic and clastic behavior.

According to Coates (10), Mohr's strength theory can be used to determine tangential and radial stresses and the radius of the zone of failed material. Ostrowski has also presented solutions to determine stresses in terms of Terzhagi's failure stress conditions for both cohesive and cohesionless (clastic) rock. Coates and Daemen (10, 55) have further developed expressions to include the liner and/or rock interaction in terms of Mohr's criteria. These relationships are relatively complex and are not included here--see the references cited for further detail.

In addition, many rock types exhibit varying degrees of time dependency. Gnirk (21) has presented solutions for viscoelastic displacement around lined and unlined shafts under uniform loading, based on four common rheological models: two-element Maxwell and Voight models, the three-element elastic model, and the four-element Burger model. Again, the referenced paper provides the detail.

In addition to the preceding discussion, failure could occur below the elastic yield point due to elastic instability by buckling or longitudinal bending. Galanka (19), Ostrowski (41), and Schlage (50) consider shaft liners as thin cylindrical shells. In addition, Coates (10) presented equations for computation of maximum compressive and tensile stress for concentrated loads on shaft linings.

For convenience in design, lining thickness may be determined by expressing Lame's equations in terms of the maximum allowable stress in the lining (σ_Θ) as follows, again assuming uniform external pressure (51, 53):

$$t = a\left(\frac{\sqrt{\sigma}}{\sigma_\Theta - 2p_o} - 1\right), \qquad (8)$$

where t = lining thickness, in,

and σ_Θ = maximum tangential stress or allowable compressive strength of the lining, psi.

A slight modification is the Huber equation (19) where

$$t = a\left(\frac{\sqrt{\sigma_\Theta}}{\sigma_\Theta - \sqrt{3}p_o} - 1\right). \qquad (9)$$

Trollope (54) developed an equation, based on Lame's analysis, to compute critical depth:

$$FZ_{(crit)} = \frac{\sigma_c}{1+2n}, \qquad (10)$$

where F = factor of safety,

Z = critical depth, ft,

σ_c = uniaxial compressive strength, psi,

and n = ratio between lateral and vertical stress, psi.

Pariseau (42) developed another equation to calculate the lining thickness in terms of critical displacement and shear modulus and to take into account the effect of face advance:

$$t = 6a\left[\left(\frac{1 - G/fG'}{1 - 2FP_o/C_o + (1-2\mu)G/fG'}\right)^{1/2} - 1\right], \qquad (11)$$

where t = lining thickness, in,

a = inner shaft diameter, ft,

F = factor of safety in compression for the lining,

G = rock shear modulus, psi,

G' = lining shear modulus, psi,

f = the relative fraction of the total displacement

$= (U-U')/U$,

U = the total shaft wall displacement that occurs with the lining installed, including U',

U' = the inward shaft wall displacement that occurs as a result of shaft sinking but before liner installation,

P_o = premining horizontal stress (applied load), psi,

C_o = unconfined compressive strength of the liner, psi,

and μ = Poisson's ratio for the rock.

The Kirsch equations, as reported by Dar (13-14), may also be further developed to express lining thickness for unequal horizontal pressure. Galanka (19) developed equations based on the maximum eccentricity in terms of the coefficient of variation of the circumferential pressure and a given lining thickness.

FINITE-ELEMENT ANALYSIS

From the preceding discussion, several shortcomings in the state-of-the-art of shaft design from a structural point of view arise, as follows:

1. The equations expressing inelastic behavior are quite complex and restricted to the conditions of a uniformly applied load and a homogeneous, isotropic, rock mass.
2. Flexibility in design is severely restricted, and investigation of design alternatives may be extremely time consuming.
3. The design and support aspects of noncircular shafts with multiple material properties have been essentially neglected.
4. The effects of excavation sequence are not considered.

The remainder of this report will illustrate the use of finite-element techniques to address some of these design shortcomings.

For a vertical shaft, a two-dimensional model must show either a horizontal or a vertical cross section. A vertical plane through the shaft centerline allows simulation of face advance, which can be used to investigate time effects and to optimize placement time of the support. A horizontal section permits analyses of cross-sectional shape, support characteristics, and orientation. A three-dimensional analysis is required to include effects of all structural parameters in a single model. This study assumes either that (1) support is installed concurrent with excavation and the applied load is irrelevant to the overall qualitative effects being analyzed or (2) a reduction in applied load simulates the appropriate load fraction applied to the support at the time of installation. A variety of models have been utilized to analyze stresses around different shaft shapes and support systems, under nonuniform loading conditions, and for elastic, plastic, and viscoelastic rock behavior.

Finite-element techniques have been applied by the Bureau, solving several large-mine-shaft-related structural problems. Pariseau (42) modeled a vertical section of a concrete-lined shaft under lithostatic loading. The liner displacement was analyzed with respect to distance above the shaft bottom. Gooch (22) monitored closure during deepening of the No. 2 shaft at the Lucky Friday Mine in the Coeur d'Alene mining district between May 1974 and April 1975. Elastic-plastic finite-element analyses were conducted, reducing the values of rock mass properties until field closure measurements generally corresponded to calculated displacements. The effect of rock bolting on stress distribution and rock yielding around the shaft was also studied.

Karwoski (30-31) studied the effect of the shape of shaft cross sections, rock anisotropy, applied stress ratios, and stress distribution around mine shafts. In conjunction with Karwoski's work, Agbabian Associates developed a finite-element computer code under a Bureau contract to solve various mining-related structural problems (18). The code is called "BMINES" and is a modification and consolidation of existing finite-element programs for solid mechanics applications. This code has been used extensively for the present study and has been recently updated (56).

DEFORMATION AND FAILURE CRITERIA

Prior to conducting finite-element analysis, the major deformational modes that may occur in the rock mass around shaft structures must be identified, including elastic, plastic, and viscoelastic. Laboratory and in situ physical property tests (7) show that the Precambrian quartzite in the Coeur d'Alene mining district primarily deforms elastically, especially within a loading range between 25 and 75 pct of the ultimate strength of the rock. It has also been noticed that rupture occurs either shortly after plastic deformation or prior to any obvious plasticity. Plastic yield zones are, therefore, identified around shaft structures as an indication of structural instability.

Viscoelastic models reveal the time effects on long-term stability of the shaft. Few data are available on time-dependent creep characteristics of the Precambrian quartzites from the Coeur d'Alene district. Operational problems with the viscoelastic option of the BMINES program at the time of this investigation resulted in only a limited amount of viscoelastic modeling.

For elastic studies, the only physical properties needed as input are bulk modulus, B, and shear modulus, G. The stress-strain relationship is indicated by

$$d\sigma_{ij} = \left(B - \frac{2}{3}G\right)d\varepsilon^{e}_{kk}\,\delta_{ij} + 2G\left(d\varepsilon^{e}_{ij}\right), \quad (12)$$

where $d\sigma_{ij}$ = the incremental stress,

and $d\varepsilon^{e}_{ij}$ = the incremental component of elastic strain.

The incremental stress-strain equation may also be expressed in matrix form as follows:

$$\{d\sigma\} = [C]\,\{d\varepsilon\}, \quad (13)$$

where $\{d\varepsilon\}$ = the total increment of strain.

The [C] matrix, therefore, contains the generalized tangent moduli and can be used in forming the element stiffness matrices. The [C] matrix may be composed of elastic segments for elastic models, or a mixture of elastic and inelastic segments for plastic models; that is, $C = C^{e} - C^{p}$. The strain-displacement relationship is expressed as

$$\{\varepsilon\} = [B]\{U\}. \quad (14)$$

For plastic deformation, a proposed yield criterion is

$$f(\sqrt{J_2}, J_1) = 0, \quad (15)$$

where $J_1 = C_1\,\sigma_{11} + C_2\sigma_{22} + C_3\sigma_{33}$, (16)

and $$\sqrt{J_2} = \frac{1}{6}\Big[C_4(\sigma_{11} - \sigma_{22})^2 + C_5\,(\sigma_{22} - \sigma_{33})^2 + C_6(\sigma_{33} - \sigma_{11})^2 + C_7\sigma_{13}^2 + C_8\sigma_{23}^2 + C_9\sigma_{12}^2\Big]^{1/2}. \quad (17)$$

A further assumption is that rock material fails in shear along planes of weakness, according to a Mohr-Coulomb failure criterion, as follows:

$$\tau = a_o - \sigma a_1, \quad (18)$$

where τ and σ = shear and normal stresses, respectively, on the plane of fracture,

and a_o and a_1 = cohesion and the angle of internal friction, respectively.

Failure may also be expressed in terms of principal stress,

$$\sigma_1 - \sigma_3 = \frac{2a_o - 2a_1\sigma_3}{a_1 - \sqrt{a_1^2 + 1}}, \quad (19)$$

with fracture occurring when

$$f = (\sigma_1 - \sigma_3) - \frac{2a_o - 2a_1\sigma_3}{a_1 - \sqrt{a_1^2 + 1}} < 0. \quad (20)$$

For viscoelastic deformation, total strain is expressed as

$$\varepsilon_t = \alpha + \beta \log t + \alpha t, \quad (21)$$

where ε_t = the total strain at time t,

α = the instantaneous elastic strain,

$\beta \log t$ = the amount of primary creep,

and αt = the amount of secondary creep.

The primary, or transient, creep expression occurs under the same load as the initial elastic strain component. Secondary or steady-state creep continues at a constant rate for a significant period of time and increases rapidly in the tertiary stage to rupture.

The overall strain rate, consisting of primary and steady-state creep, $\frac{d\varepsilon}{dt}$, is also related to the applied load, σ, and the coefficient of viscosity of rock, η, as

$$\frac{d\varepsilon}{dt} = \frac{\sigma}{\eta}. \qquad (22)$$

Kelvin and Maxwell models are utilized to characterize viscoelastic behavior in more detail. The creep strain for the Kelvin model is expressed as

$$\varepsilon^c_{t + \Delta t} = \varepsilon^c_t \exp(-\alpha_1 \Delta t) + \sigma_t \frac{\alpha_2}{\alpha_1}\left[1 - \exp(-\alpha_1 \Delta t)\right], \qquad (23)$$

where $\alpha_1 = \frac{B}{\eta_B}$ and $\alpha_2 = \frac{1}{\eta_B}$ represent creep in volumetric strain,

and $\alpha_1 = \frac{G}{\eta_s}$ and $\alpha_2 = \frac{1}{\eta_s}$ represent creep in shear strain.

The creep strain for the Maxwell model is expressed as

$$\varepsilon_{t + \Delta t} = \varepsilon^c_t + (\alpha_2 \Delta t + \alpha_1)\sigma_{t + \Delta t} - \alpha_1 \sigma_t, \qquad (24)$$

where $\alpha_1 = \frac{1}{B}$ and $\alpha_2 = \eta_B$ represent creep in volumetric strain

and $\alpha_1 = \frac{1}{G}$ and $\alpha_2 = \eta_s$ represent creep in shear strain,

where η_B and η_s = bulk and shear coefficients of viscosity, respectively,

and t = time.

ANALYTICAL CONSIDERATIONS

The basic approach towards finite-element modeling in this study is to use representative input data based on actual measurements made in the field. Input of actual field conditions lends credibility to the results, as opposed to a parametric-type analysis. Several considerations regarding field, or "fixed," conditions, "variable" design parameters, and failure criteria as used in this study must be defined.

The magnitude and direction of in situ principal stresses, the ratio between horizontal stresses, and major geological features such as rock type, bedding, and major planes of weakness or fracture are considered as "fixed" conditions and cannot be changed by the designer. The size, shape, and orientation of the shaft, the type and dimension of shaft support, and the time of placing permanent support are "variable" parameters; that is, they can be altered during design or construction to provide the most stable condition. To encompass the complete range of rock mass deformational modes, the elastic, plastic, and viscoelastic options of the "BMINES" code were used. These behavioral modes are expressed in equations 12 through 21. Other considerations follow:

1. The depth of the shaft, relative to the shaft cross section, is infinite; two-dimensional, horizontal, plane strain conditions are assumed.

2. For evaluation of the effect of the horizontal stress ratio, input loads to the model boundaries range from 1:1 to 3:1, to cover the range of measured field stresses.

3. Shaft excavation and support installation occur simultaneously to simulate a "worst case" loading condition. In actuality, support installation often lags shaft excavation by several days; however, for a two-dimensional elastic analysis, the stress increment applied to the support system changes only the relative magnitude, and not the nature, of the rock-support interaction.

TABLE 3. - Material property input parameters for finite-element analysis

Materials	Modulus of elasticity (E), psi	Poisson's ratio (μ)	Bulk modulus (B), psi	Shear modulus (G), psi
Hard quartzite	10,000,000	0.25	6,666,700	4,000,000
Lucky Friday Mine quartzite	8,100,000	.205	4,576,270	3,361,000
Caladay Project quartzite	9,570,000	.205	5,406,800	3,971,000
Argillite	1,000,000	.25	666,670	333,340
Concrete:				
3,000-psi strength	3,140,000	.15	1,495,240	1,365,220
4,000-psi strength	3,620,000	.15	1,723,809	1,573,913
5,000-psi strength	4,050,000	.15	1,928,570	1,760,870
9,000-psi strength	5,407,500	.15	2,575,000	2,351,000
Carbon steel	30,000,000	.3	25,000,000	11,538,461
Douglas fir timber	1,900,000	.25	1,260,000	760,000
Sand	2,000	.15	952	870

4. Physical properties of the mine rocks used for material property input represent certain groups of Precambrian quartzite tested in situ and/or in the laboratory. Table 3 lists typical physical properties for various materials used in this analysis.

5. Circular, rectangular, and elliptical shaft cross sections are simulated. Since all have axes of symmetry, only a quarter of the cross section with the opening and adjacent rock mass requires modeling.

6. Stress concentration factors are used to evaluate relative effects of anisotropy and support performance. The ratio of tangential stress, or "perimeter" stress in the case of rectangular openings, to applied stress defines stress concentration.

7. Axial displacement is used as a stability criterion in analyzing the effects of geologic discontinuities and support systems for rectangular openings.

8. Plastic yield factors are used to indicate whether yielding has occurred in an element (from equations 15-20). The yield factor is derived from the Mohr-Coulomb failure criterion requiring input of rock strength, cohesion, and internal friction.

CIRCULAR SHAFTS

It has been well documented that the stress concentration factor around a circular opening for unidirectional loading conditions is -1 for the roof position and +3 in the rib. For example, if a circular tunnel has only compressive loading from overburden, the internal peripheral stress at the crown point is the same as the overburden load, but in tension and at the spring line, the rock is subjected to a compressive load three times the overburden load. Under hydrostatic conditions, that is, applied loads equal in all directions, the stress concentration is 2 at any position on the opening boundary, obviously a condition favorable for a circular shape.

To illustrate the influence of applied stress ratio, and to compare finite element method (FEM) results with conventional closed-form solutions, a basic two-dimensional, 14-ft-diam, circular shaft was modeled. Figure 4 shows details of the model, which has 280 elements and 315 nodal points. The bulk and shear moduli of the rock are 6.7×10^6 psi and 4.0×10^6 psi, respectively, representing very hard, brittle quartzite (table 3). Three sets of applied stresses, with a (p_x/p_y) of 6,000/2,000, 6,000/3,000, and 6,000/6,000 psi, were used as input loads on the model boundary, 7 radii from the center of the opening. These values are typical

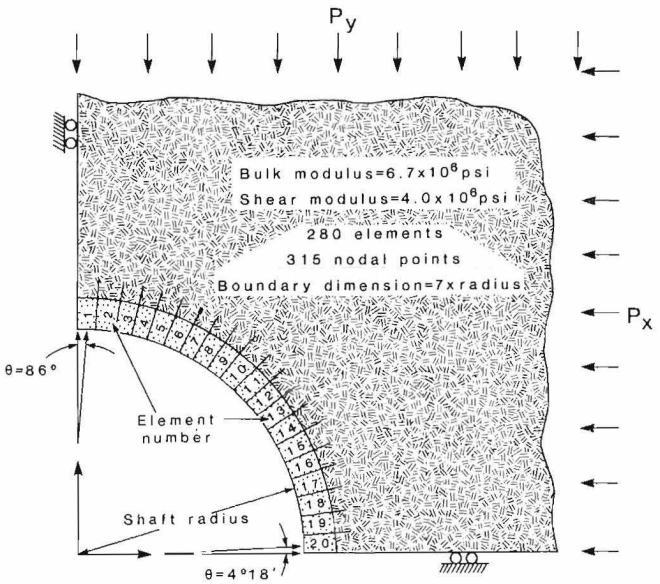

FIGURE 4. - Finite-element model for analysis of circular shaft.

of the range of stress magnitudes and ratios determined in the field (tables 1 and 2).

The first 80 to 160 elements nearest the shaft opening (fig. 4) simulate varying thicknesses of concrete lining with a bulk modulus of 1.7×10^6 psi and a shear modulus of 1.0×10^6 psi. The remaining elements represent the rock mass surrounding the shaft.

Figure 5 clearly illustrates the effect of the stress ratio in terms of the maximum tangential stress. At a 3:1 or greater stress ratio, a circular opening would become unstable as the tangential stress nears the yield point of weaker quartzites. Conversely, the 1:1 loading condition is the most favorable, showing a uniform stress throughout.

Comparison of these results with those calculated using the Lamé and Kirsch solution (equations 2 and 6) shows an approximate ±5 pct difference. The closed-form solutions are exact; the discrepancy in the finite-element results is due to the stress being calculated at the center of the element instead of exactly at the opening boundary. However, a finer mesh near the opening would minimize this difference. In figure 5, the 1:1 loading condition results in a stress concentration factor of 1.93, versus 2 for an exact solution. For the 3:1 loading condition, the maximum tangential stress normal to the direction of maximum applied stress is 2.7 times the applied stress, versus 3 for the exact solution.

Element 1 at the $\Theta = 90°$ position reaches a maximum of over 16,000 psi and becomes tensile element 20 at the $\Theta = 0°$ position. For an applied stress ratio of 6,000/3,000, the tangential stress in element 1 is slightly below 16,000 psi in element 1 and a little higher than 2,500 psi in element 20, both compressive. For the 1:1 condition, all tangential stresses are the same, or slightly lower than 12,000 psi.

Figure 6 shows the relative effect of a 2-ft thickness of concrete if installed immediately upon excavation of the rock. The tangential stress at the concrete-rock interface is reduced by 21 pct for a 3:1 applied stress ratio and by 17 pct for a 1:1 condition. Figure 7 shows the corresponding tangential stress on the concrete surface for a 3:1 applied stress ratio for various thicknesses. Note that the stress developed in the concrete increases slightly with increasing thickness. A tensile zone also exists in the concrete on approximately 20 pct of the periphery.

These results show that if the concrete liner was installed immediately upon excavation, the resulting decrease in displacement-induced stress concentration in the rock would be significant. Concrete thickness appears to have only minimal effect on resulting stress levels in the concrete. In fact, a slight increase in stress is seen owing to the greater excavation of rock material and subsequent larger displacement.

Plastic analyses were also conducted to determine the yield zones for unsupported and concrete-lined circular shafts at varying stress ratios. This enables determination of failed zones according to the Mohr-Coulomb yield criteria, as

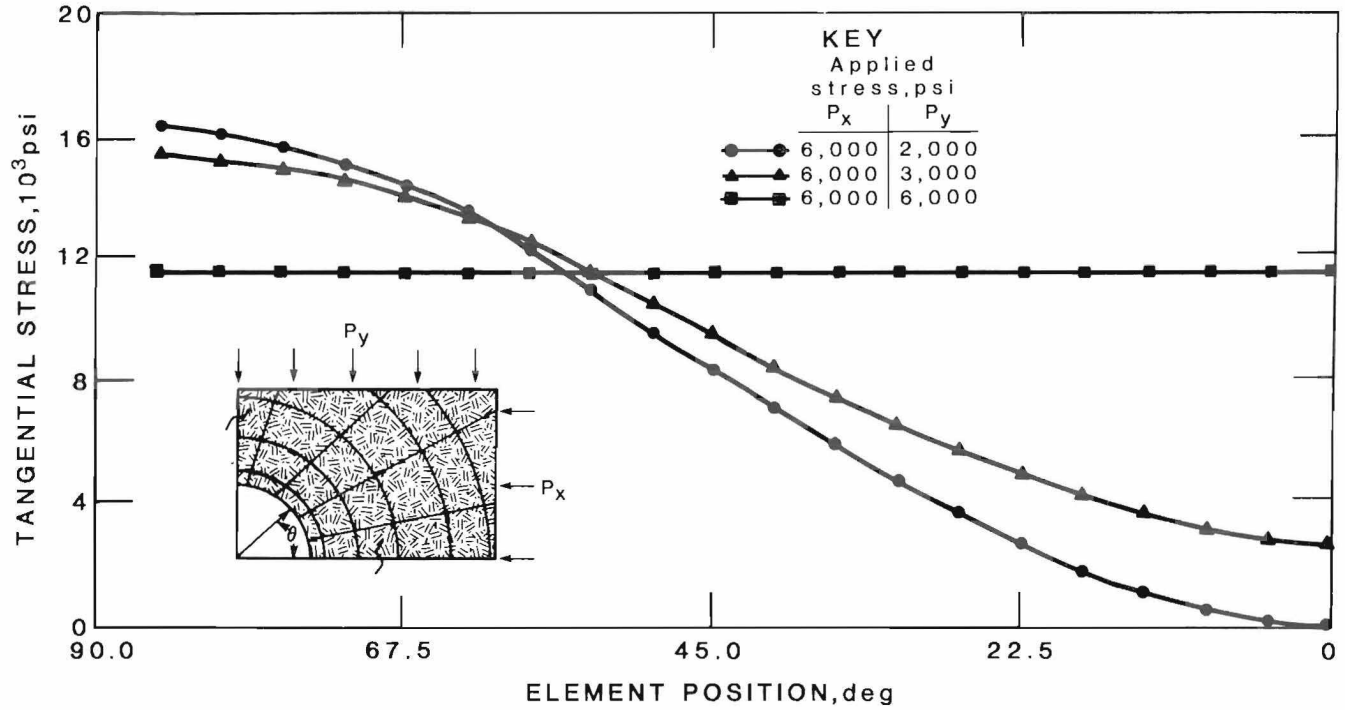

FIGURE 5. - Tangential stress distribution around 14-ft-diam unsupported shaft as function of stress ratio.

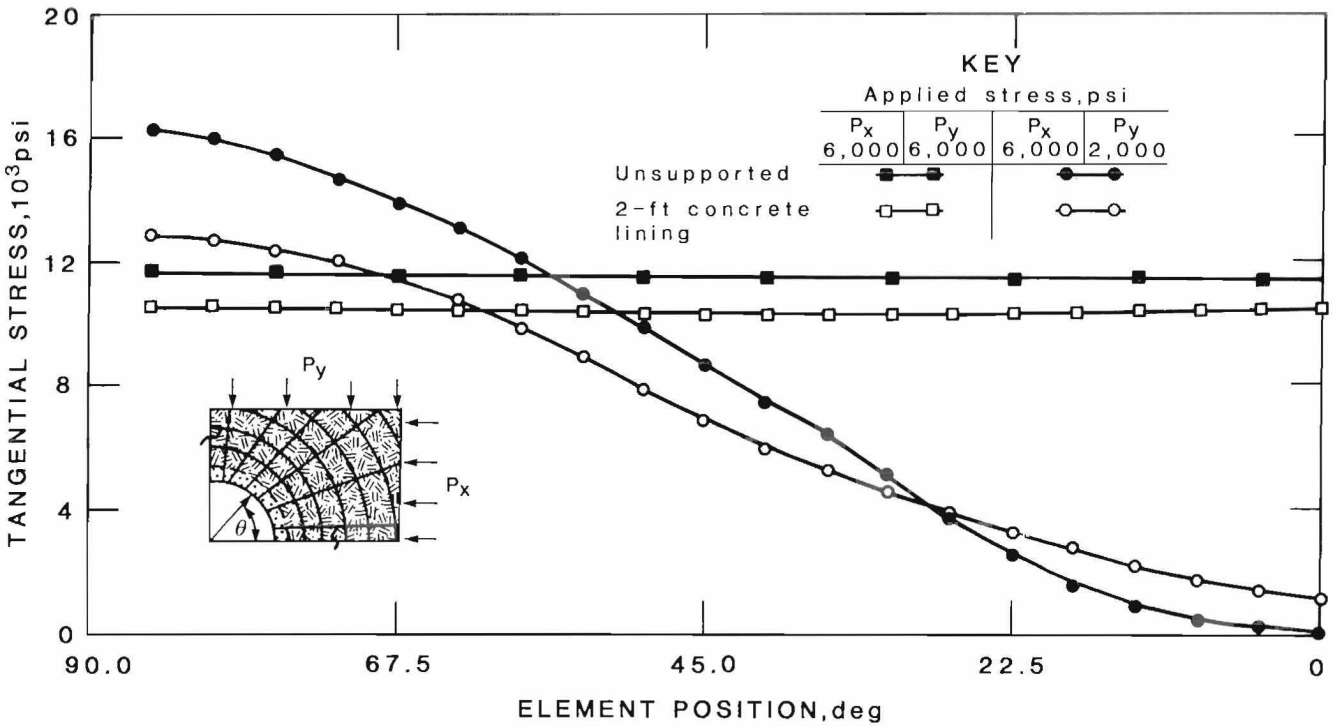

FIGURE 6. - Tangential stress distribution in rocks around 14-ft-diam supported and unsupported shafts.

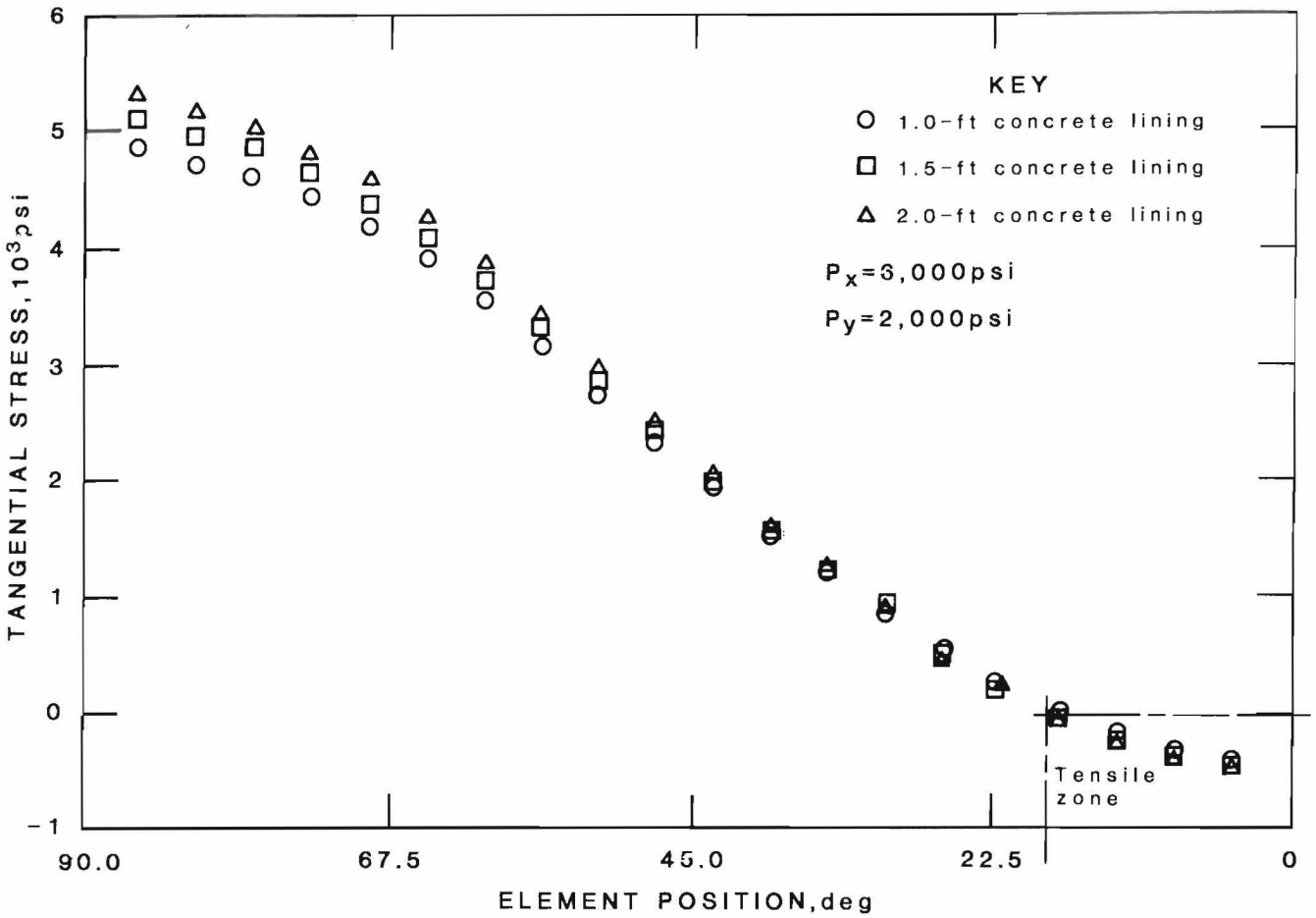

FIGURE 7. - Tangential stress distribution for various thicknesses of concrete lining for 14-ft-diam shaft.

expressed by equations 17, 18, and 19. As indicated from typical unconfined and triaxial stress-strain curves for quartzites (7), the rock deforms elastically over a wide range, and plastic deformation occurs only shortly before rupture. Therefore, the occurrence of plastic yielding is almost simultaneous with the elastic yield point. The plastic model is similar to the elastic model, and yielded elements are shown with the yield zone. Figures 8*A*, 8*B*, and 8*C* show yield zones around unsupported 14-ft-diam circular shafts for 3:1, 2:1, and 1:1 applied stress ratios, respectively.

Figure 8*A* indicates that the plastic yield zone around the unsupported circular shaft for an applied load of P_x = 6,000 psi and P_y = 2,000 psi is located on the shaft perimeter 90° from P_x, the maximum stress, and extends about 6 in into the rock. When the applied load changes to P_x = 6,000 psi and P_y = 3,000 psi, seven elements in the first layer (3 in) yield plastically (fig. 8*B*). If the applied load is a uniform 6,000 psi, the inside ring of elements, representing a 3-in rock layer, yields plastically (fig. 8*C*). The actual failure mode might be an elastic instability such as shell buckling or cylinder crushing. The plastic analyses show that rock material can be expected to yield and fail in hard brittle quartzites for typical load levels and stress ratios experienced in deep shafts. In fact, as mentioned previously, several circular raise bores in the Couer d'Alene mining district have developed failure geometry reflecting the yield zones shown by figures 8*A* and 8*B*, which indicates a biaxial stress condition.

Figures 9*A*, 9*B*, and 9*C* show the plastic yield zones around a 14-ft-diam shaft lined with 1, 1-1/2, and 2 ft of concrete, respectively, with an applied stress ratio of 3:1. Comparing figures 9*A* and 8*A*, the depth of yield in the rock is decreased owing to the liner. However, extensive yielding might occur in the concrete, which may or may not be significant, depending on accompanying displacement. With increasing concrete thickness, figures 9*B* and 9*C* show that the yield zone in the rock mass is eliminated. The concrete shows slightly more yield owing to the increased rock excavation required. This shows that the effect of concrete thickness as a support variable is minimal.

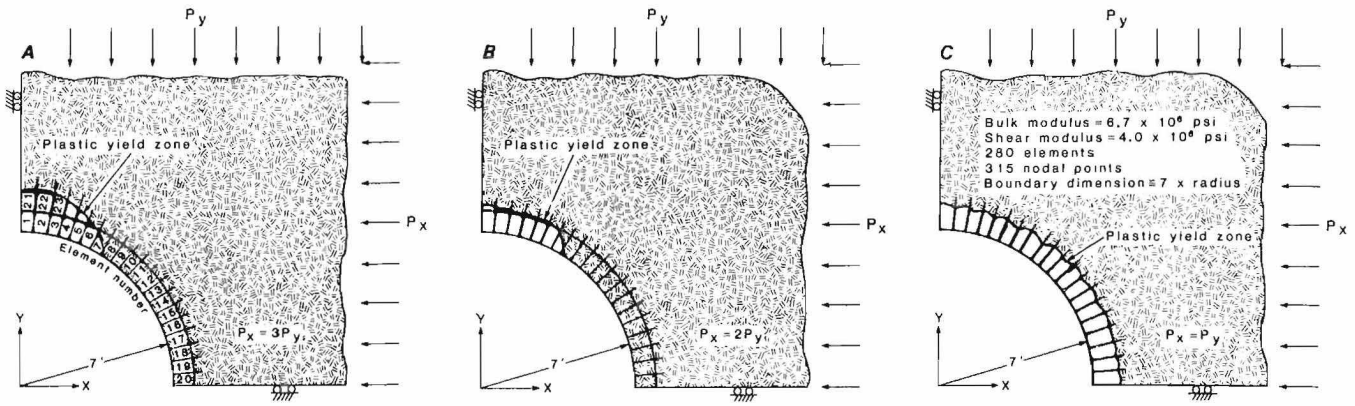

FIGURE 8. - Plastic yield zones around unsupported, 14-ft-diam shaft. *A*, 3:1 applied stress ratio; *B*, 2:1 applied stress ratio; *C*, 1:1 applied stress ratio.

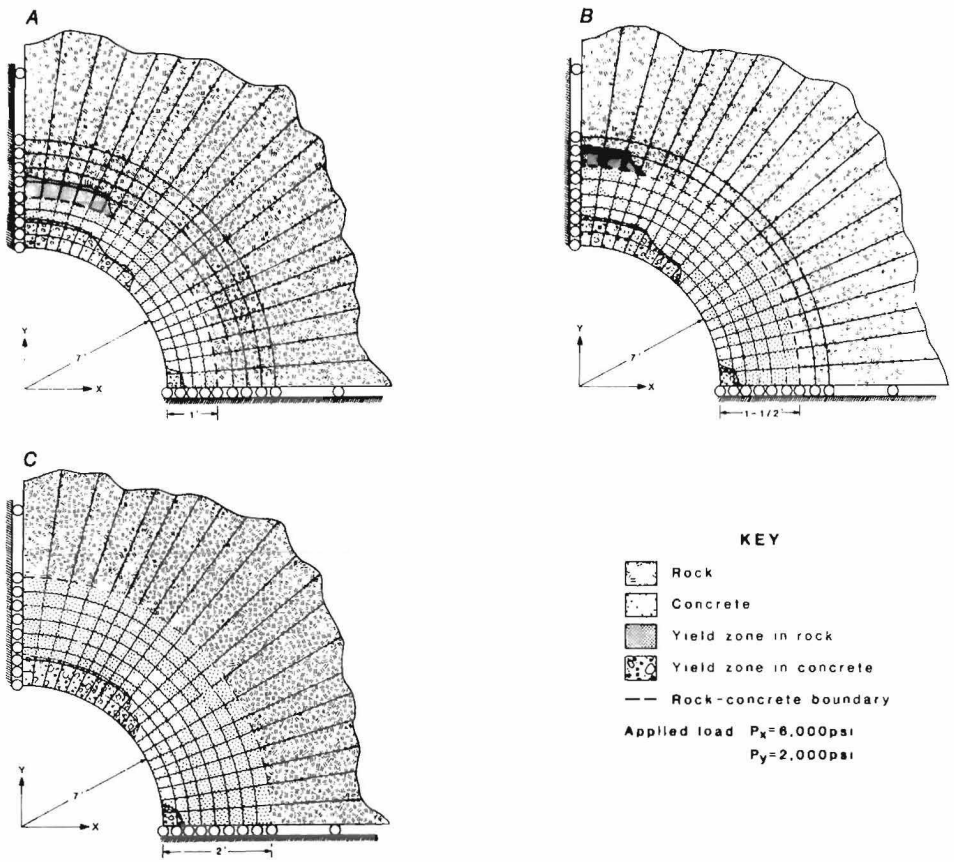

FIGURE 9. - Plastic yield zones around supported, 14-ft-diam shaft at a 3:1 stress ratio. *A*, 1 ft of concrete; *B*, 1-1/2 ft of concrete; *C*, 2 ft of concrete.

RECTANGULAR SHAFTS

A rectangular shaft opening presents a more difficult configuration for a designer. The orientation with respect to the prevailing stress field, as well as local geologic discontinuities, must be taken into consideration. As discussed previously, the traditional design approach has been to orient the short axis parallel with the strike of prevailing weakness planes, which in most cases is bedding. The long side of the shaft will thus intersect the rock normal to the weakness planes, minimizing their effect and exposure in the shaft wall. However, the in situ prevailing stress field complicates the effect of geologic discontinuities, particularly if stress levels exceed rock strength.

EFFECT OF STRESS RATIO AND ORIENTATION

To illustrate the significance of the stress ratio and shaft orientation, a two-dimensional cross-sectional model simulating one-fourth of a 10- by 20-ft, unsupported, rectangular shaft was analyzed. This model has 168 elements and 199 nodal points. The rock is medium-hard quartzite having the following material properties:

Bulk modulus (β).....10^6 psi..	5.407
Shear modulus (G).....10^6 psi..	4.0
Angle of internal friction (ϕ) deg..	52
Cohesion (c).....psi..	2,836
Angle of failure plane.....deg..	60
Modulus of elasticity..10^6 psi..	9.57
Poisson's ratio.....	0.21

Plastic analysis was conducted to determine the yield zones due to various applied stress fields. Figure 10 shows the effects for stress ratios of unidirectional, 3:1, 2:1, and 1:1 conditions with the major axis aligned both parallel and normal to the major stress. The shaded elements illustrate the potential yield zones in the rock mass for that particular set of applied stresses.

Figure 10*A* shows yield zones around an unsupported shaft for a unidirectional stress field with the major axis alined parallel to the major stress. The unidirectional condition might occur when a shaft penetrates an area that has nearby mined-out zones, and the stress in one direction is very large with respect to stress in the other direction. General yielding occurs along the short axis of the shaft, radiating out from the corners with compressive failure; the short wall exhibits tensile failure. This is a particularly realistic condition when the vein structure parallels bedding and nearby mining results in unidirectional loading normal to bedding planes, causing "beam bending" type failures.

With stress normal to the long axis (fig. 10*B*), even more extensive yielding occurs and extensive shaft instability would result. If bedding planes or other major discontinuities were also parallel with the long axis, this loading condition would be particularly severe, resulting in the worst combination of applied stress ratio and orientation for the rectangular shape.

With a stress ratio of 3:1 and the maximum load parallel with the long axis (fig. 10*C*), shaft stability is greatly improved. Almost no yielding occurs except near the corner, this area soon becoming stable as the corner yields and becomes rounded. In addition, excavation practices would produce an irregular, somewhat rounded, corner which would smooth out the sharp increase in stress. This is the most desirable of all combinations of applied stress ratio and orientation, and if major weakness planes also were oriented normal to the long axis, maximum stability would result. In contrast, figure 10*D* shows this stress ratio rotated 90°, and extensive yielding still occurs around the shaft. The long shaft wall would be subject to tensile failure (beam bending), while the short wall would be subject to high compressive stress.

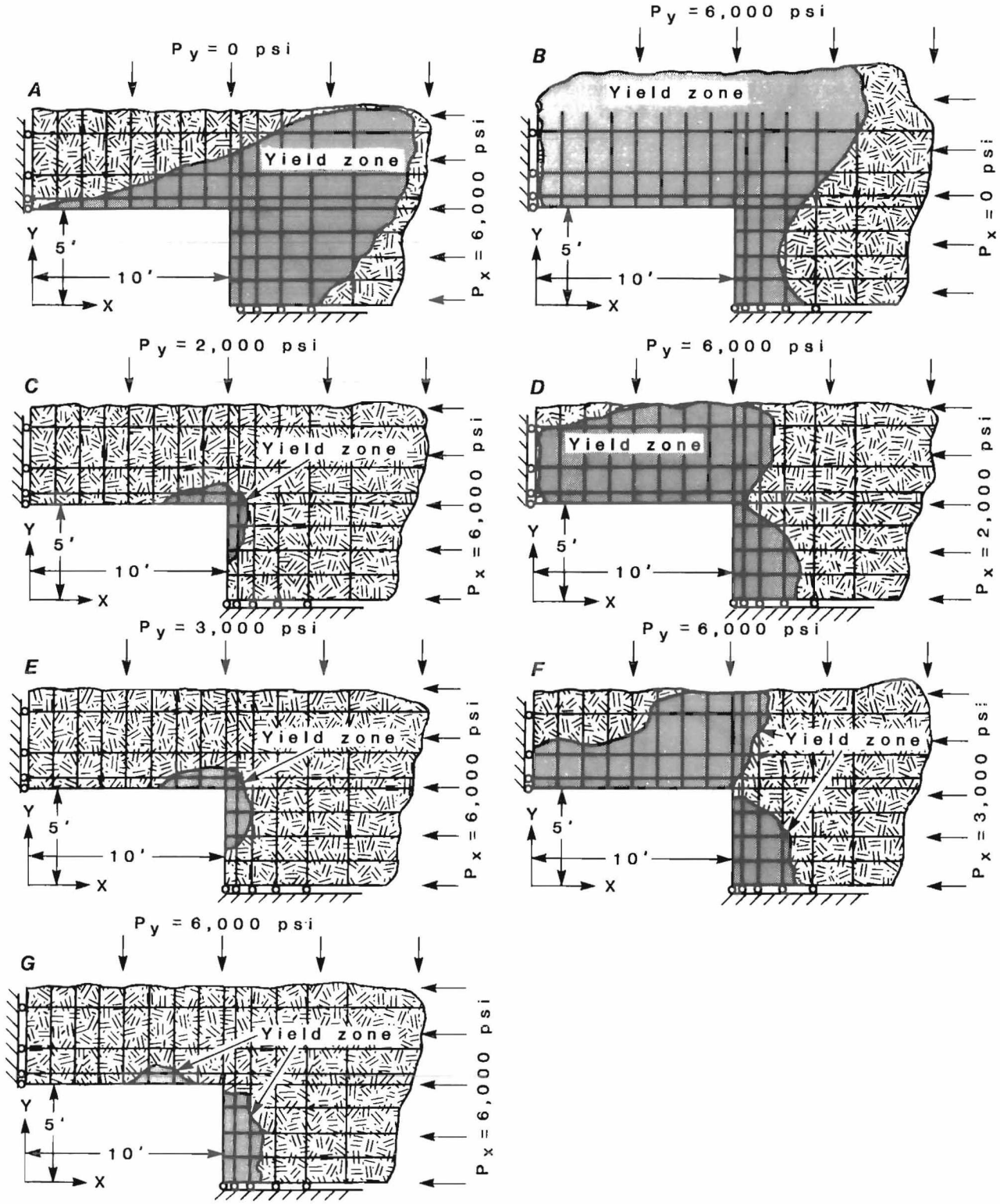

FIGURE 10. - Plastic yield zones around unsupported 10- by 20-ft rectangular shafts for varying stress ratios. *A*, Unidirectional stress parallel with major axis; *B*, unidirectional stress normal to major axis; *C*, 3:1 stress ratio with minimum stress parallel with long axis; *D*, 3:1 stress ratio with maximum stress normal to long axis; *E*, 2:1 stress ratio with maximum stress parallel with long axis; *F*, 2:1 stress ratio with maximum stress normal to long axis; *G*, 1:1 stress ratio.

This trend continues in figures 10*E*, 10*F*, and 10*G*. Almost no yielding appears in figure 10*E* at a 2:1 stress ratio with the major stress parallel with the long axis. However, in figure 10*F*, with major stress normal to the long axis, considerable yielding again occurs. Figure 10*G* shows the 1:1 loading condition with fairly severe yielding at the midpoint of the short wall.

In general, the best combination of applied stress and shaft orientation is with the major stress parallel with the long shaft axis. The worst case is unidirectional loading, regardless of orientation, or with major stress normal to the long wall of the shaft. As the major stress rotates from parallel with the long axis of the shaft to normal to the long wall, the yield zones increase accordingly. Furthermore, increasing stress magnitudes obviously increase the zone of yielding and the extent of unstable ground around the shaft. Little can be done to alter the stress field, but the optimum orientation can be determined during the design stages.

A notable departure of the preceding analysis from classical elastic solutions is the lack of high-stress conditions in the corners of the shaft and, thus, development of "critical stresses." This is attributed to the confining effect of adjacent sides, resulting in higher effective strength. Plastic yielding in this area is further restrained as blocking points for timber or steel sets are installed. In addition, the coarse mesh of the model prevents resolution of highly localized stresses, and yield levels are extrapolated from the trend of the stress on either side.

GEOLOGIC DISCONTINUITIES

Geologic discontinuities, such as bedding planes, joints, faults, etc., also affect the stability of a shaft, particularly where these defects are steeply dipping. The resulting situation is that the vertical shaft wall intersects the discontinuity at a relatively small angle, and, consequently, the plane of maximum shear stress often coincides with preexisting weakness planes.

The rock masses in deep mines, such as in the Coeur d'Alene District, are not homogeneous bodies. They consist of interbedded and, often, intensively fractured and folded formations. A typical lithological feature is interbedded quartzite and argillite. The quartzite beds are usually hard, brittle, and medium to thick; the argillites are soft, weak, and thinly bedded. Physical properties of argillaceous material are largely unknown; however, a modulus value of one-tenth that of intact quartzite that has been used in previous work (7, 43) is used in these analyses. Two finite-element models simulating a simple quartzite-argillite interbedding condition have been analyzed. The following input data were utilized:

Bulk modulus (quartzite)...10^6 psi..	6.7
Shear modulus (quartzite)...10^6 psi..	4.1
Applied load (Px = Py).....psi..	3,000

Figure 11 shows bedding parallel with the long axis, and figure 12 shows it normal to the long axis. Figure 13 shows tangential stress concentration around a rectangular shaft for these two conditions of interbedding, compared to the case of a shaft located in 100 pct quartzite. The loading condition is uniform to minimize the influence of the stress ratio. The stress distribution is keyed to the element notation in figures 11 and 12.

Little difference in stress concentration around the shaft perimeter exists for the all-quartzite model and interbedding parallel to the long axis. Tangential stress concentration is severe along the short axis and corners of the shaft if bedding is normal to the long axis.

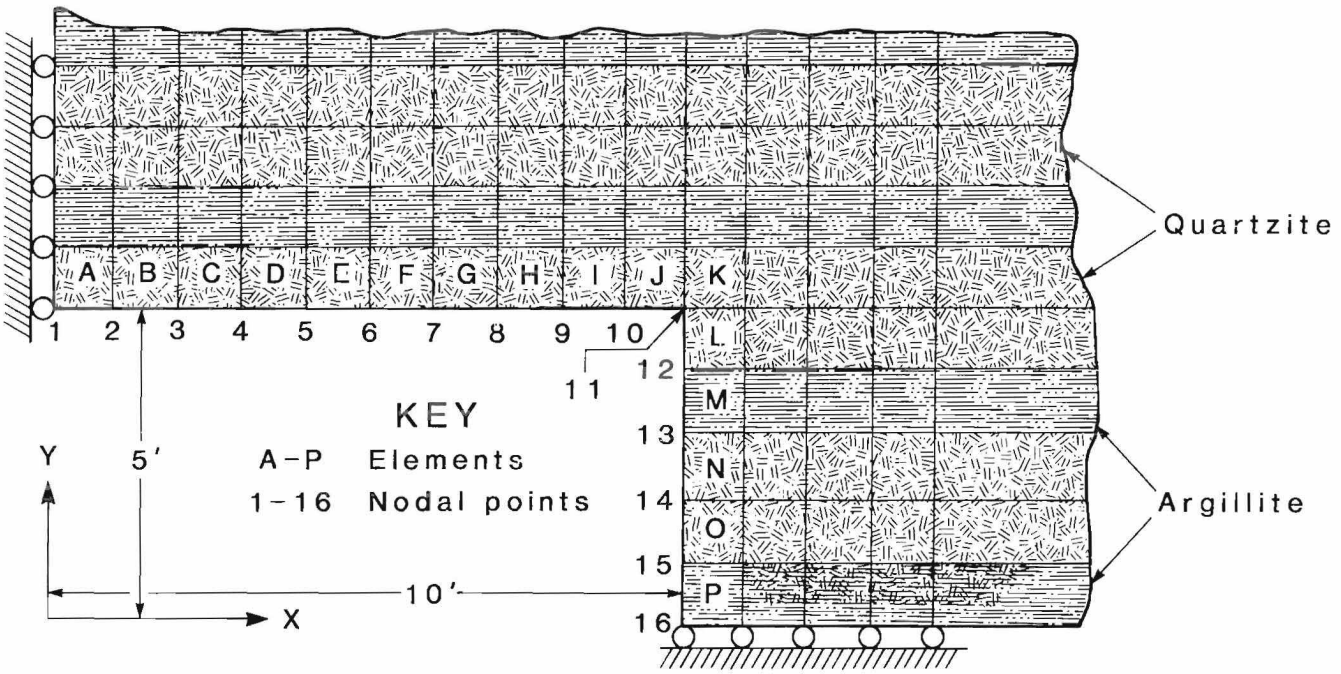

FIGURE 11. - Model of interbedded quartzite and argillite striking parallel with long axis of shaft.

Figure 14 shows the displacement distribution keyed to the nodal point notation in figures 11 and 12. The greatest axial displacement occurs at the midpoint of the long dimension for the interbedded condition paralleling the long axis and is almost three times greater than if no argillite was present. The axial displacement is also more than twice as great at this position for bedding normal to the long axis. Displacement along the short axis is not significantly affected by bedding parallel to the long axis. However, it is about four times as great for normal bedding. In general, the tangential stress and magnitude of axial displacement are considerably greater for the condition of interbedded quartzite and argillite than for quartzite alone.

Other typical geologic discontinuities which exist are jointing systems and fault blocks. Analysis was conducted to examine these effects on stability of rectangular shafts. Open fractures, simulating a faulted structure infilled with gouge material, were analyzed with zero cohesion and with no frictional resistance to shear along the plane of weakness. Tight fractures simulated joints where little or no lateral movement has occurred and cohesion and internal frictional resistance remain. Figure 15 shows the two-dimensional model used for fracture analysis. One to three evenly spaced fractures oriented either normal or parallel to the long axis of the shaft, and extending into the rock mass to the boundary of the model, were simulated.

Models were loaded uniformly to 3,000 psi with a bulk and shear modulus of 6.7×10^6 psi and 4.0×10^6 psi, respectively. Figure 16 shows axial displacement along the long axis for an open-fracture system oriented normal to the long axis. Displacement at the midpoint of the long wall ranges from negligible in unfractured material to almost 5 in for the three-fracture system.

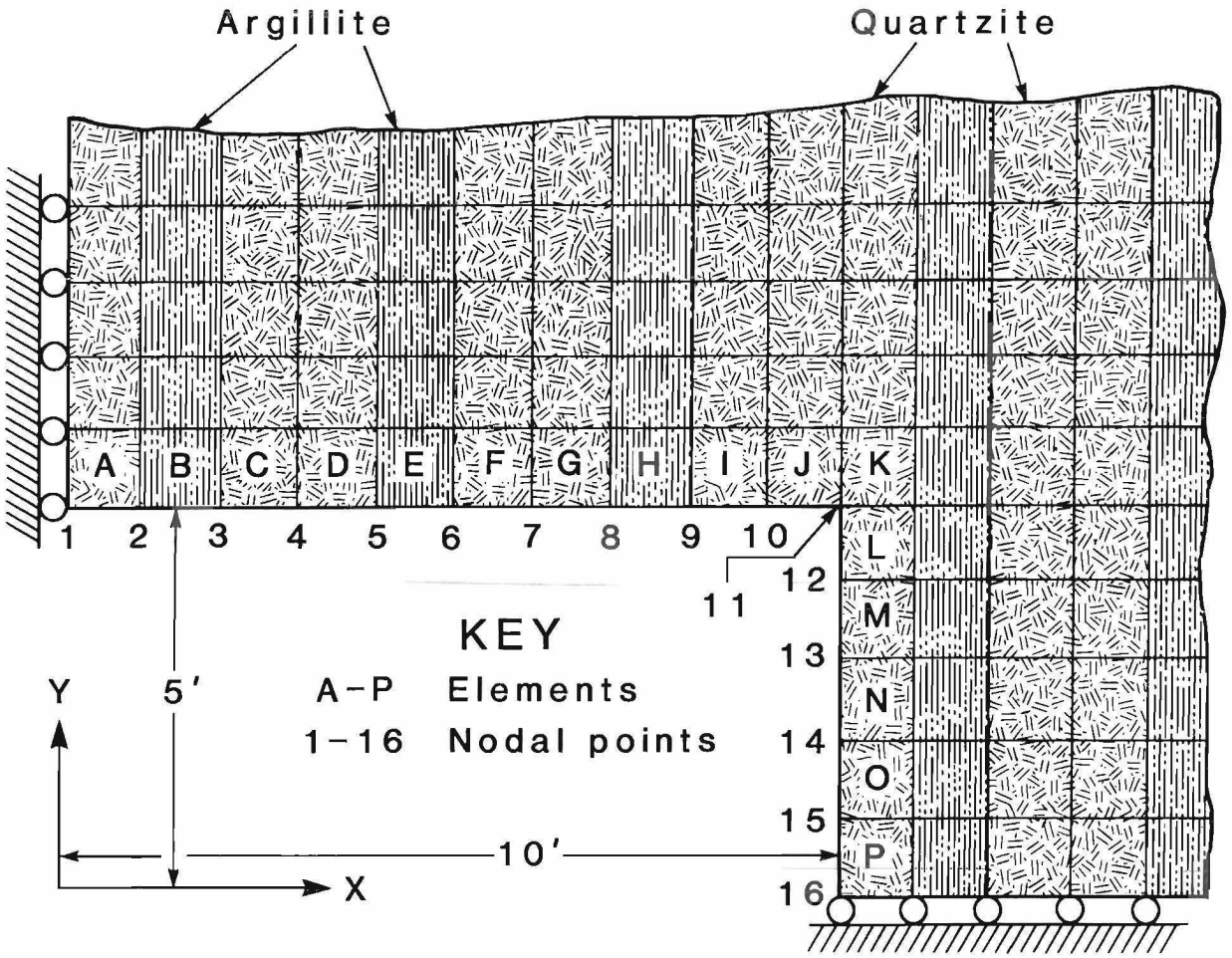

FIGURE 12. - Model of interbedded quartzite and argillite striking normal to long axis of shaft.

Figure 17 shows axial displacement when a tight fracture is simulated. Maximum axial displacement is again along the long axis at the midpoint. However, the magnitude is less than one-half that of the open-fracture system. Rock mass properties thus have a significant influence on the deformational behavior of the shaft walls.

SHAFT SIZE AND SUPPORT SYSTEM

Design parameters that may be considered variable and also affect structural behavior of rectangular shafts are the size, the length-to-width (L/W) ratio of the axes, and the support system. To determine wall displacement and stress concentration as a function of shaft size and dimensions, an unsupported rectangular shaft with the L/W ratio varying from 1.6 to 2.5 was analyzed. The short axis was fixed at 10 ft, to decrease the number of variables, and the length of the long axis was varied. Rectangular shafts from 10 by 16 ft to 10 by 25 ft were modeled, typical of shafts constructed in deep mines. The model cross section contains 400 elements and 446 nodal points. Bulk and shear modulus is 5.4×10^6 psi and 3.6×10^6 psi, respectively.

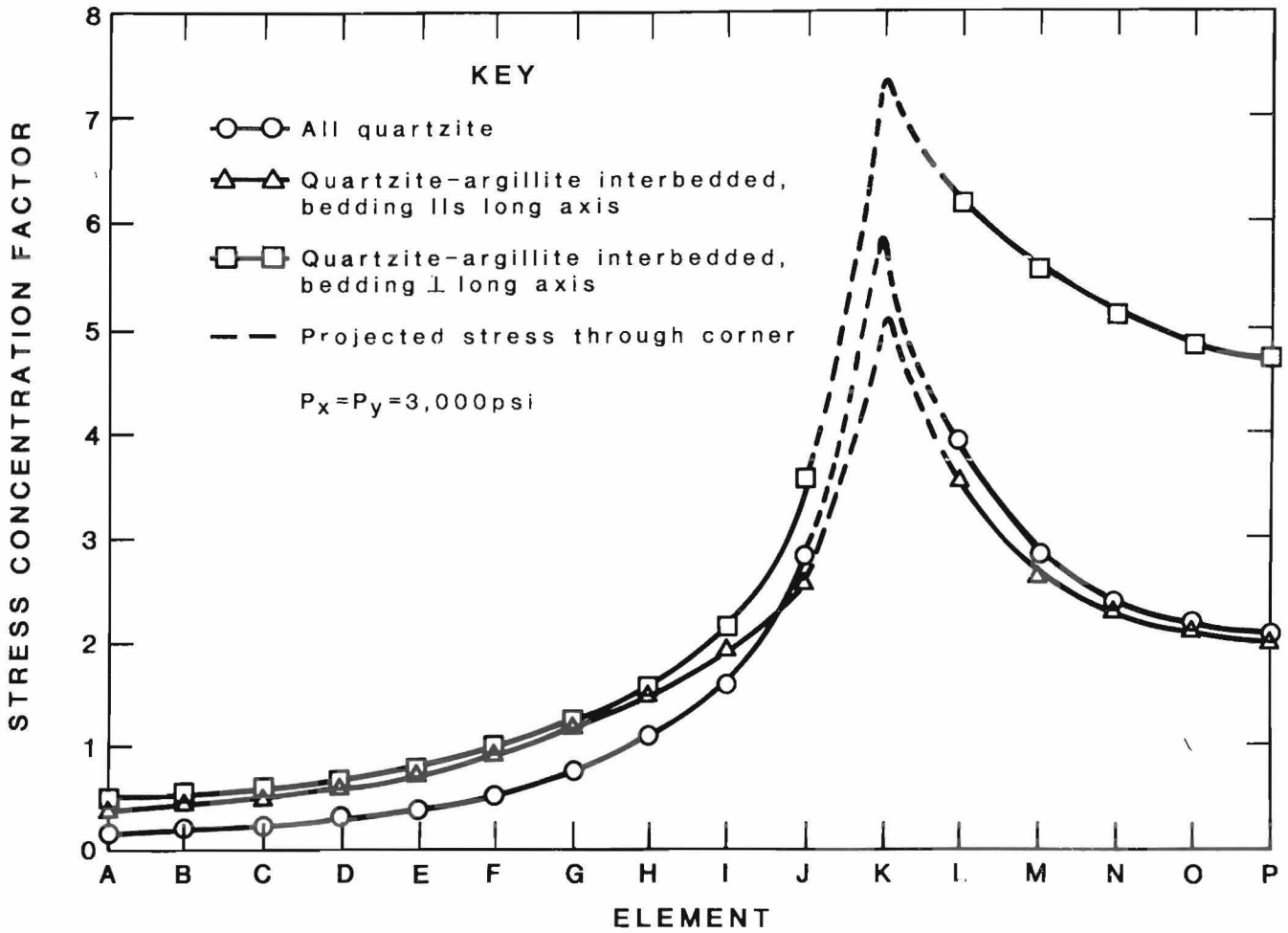

FIGURE 13. - Stress concentration factor around 10- by 20-ft rectangular shaft in layered rocks.

Figures 18*A*, 18*B*, and 18*C* show stress concentration around the shaft perimeter for varying L/W ratios and uniform and biaxial stress fields. Figure 18*A* illustrates the stress concentration for a 1:1 loading condition. This figure shows that as the shaft length increases with respect to its width (fixed at 10 ft), the stress decreases along the long side and increases along the short side. A 50-pct increase in length changes the maximum stress concentration by about 30 pct. As the stress becomes more strongly biaxial with the major stress acting parallel to the long axis, the preferred orientation, the change in stress concentration becomes less pronounced with increasing L/W, as shown in figures 18*B* and 18*C*.

Figure 19 shows the maximum axial displacement occurring as a function of the L/W ratio for varying stress ratios. In all cases, the maximum displacement is at the midpoint of the long side and, contrary to tangential stress, is strongly dependent on L/W ratio. A uniform loading condition results in the most significant effect, with a 60-pct increase in L/W more than doubling the displacement. The effect of increased L/W is lessened as the stress ratio becomes biaxial, with the maximum being parallel with the long axis. The effect on displacement at the midpoint of the short axis is minimal for all loading conditions.

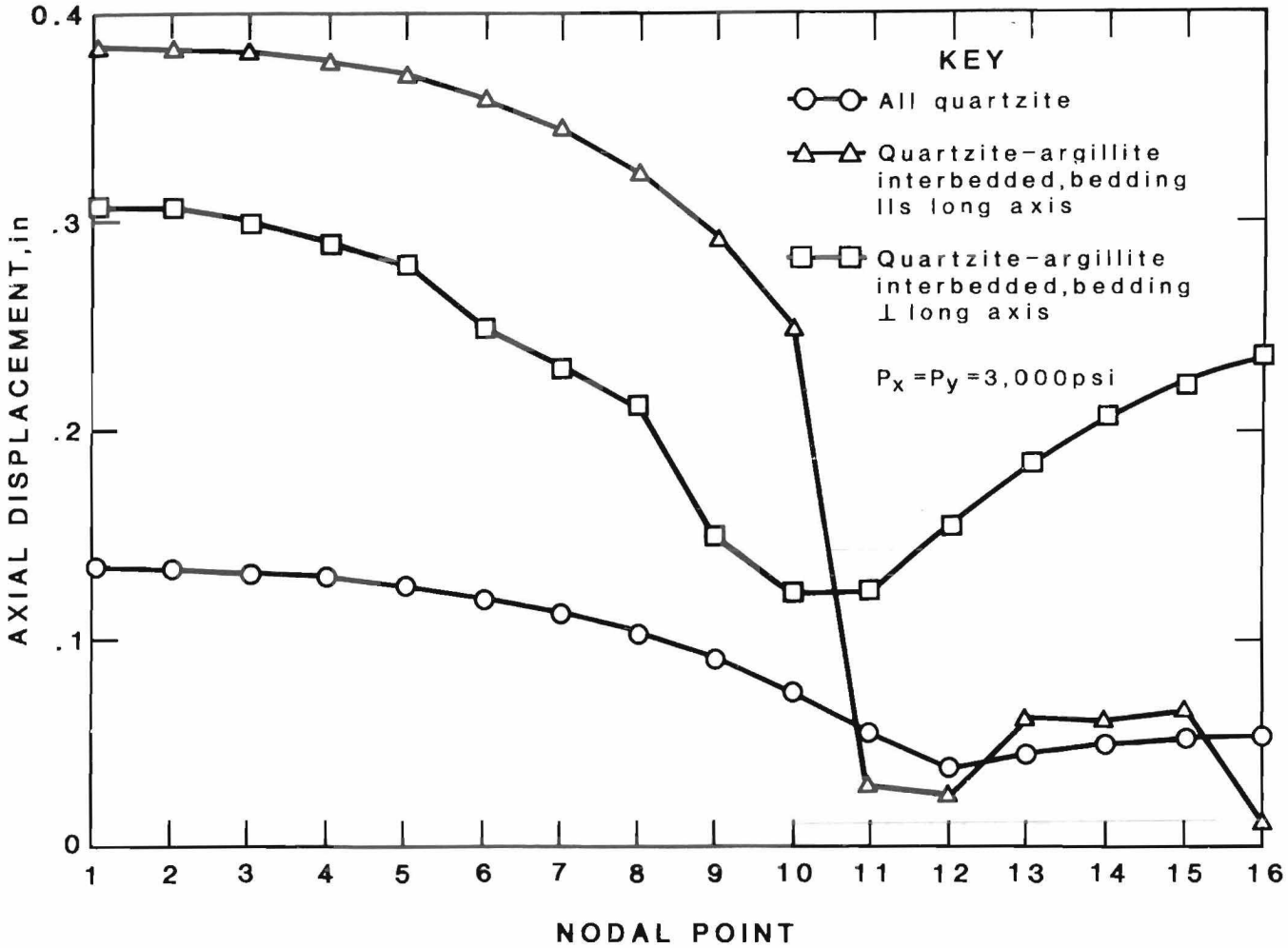

FIGURE 14. - Axial displacement around 10- by 20-ft unsupported rectangular shaft in layered rocks.

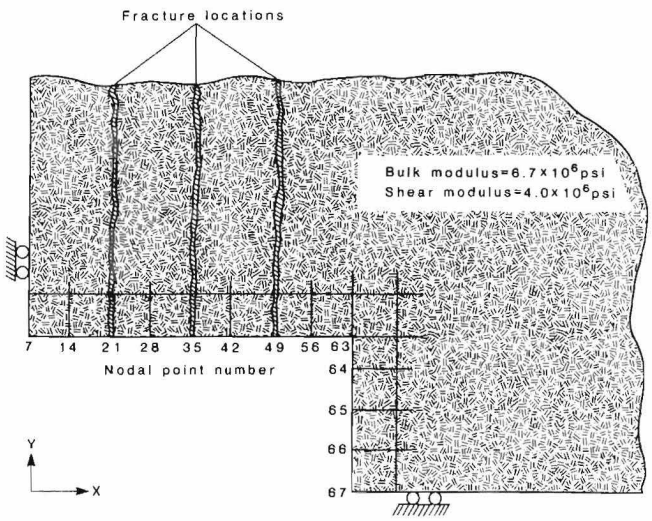

FIGURE 15. - Model used for fracture analysis for 10- by 20-ft rectangular shaft in hard quartzite.

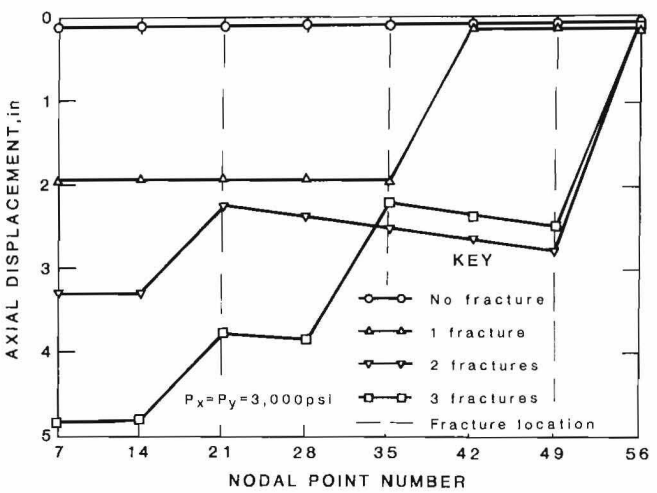

FIGURE 16. - Axial displacement along long edge of 10- by 20-ft rectangular shaft with open fractures.

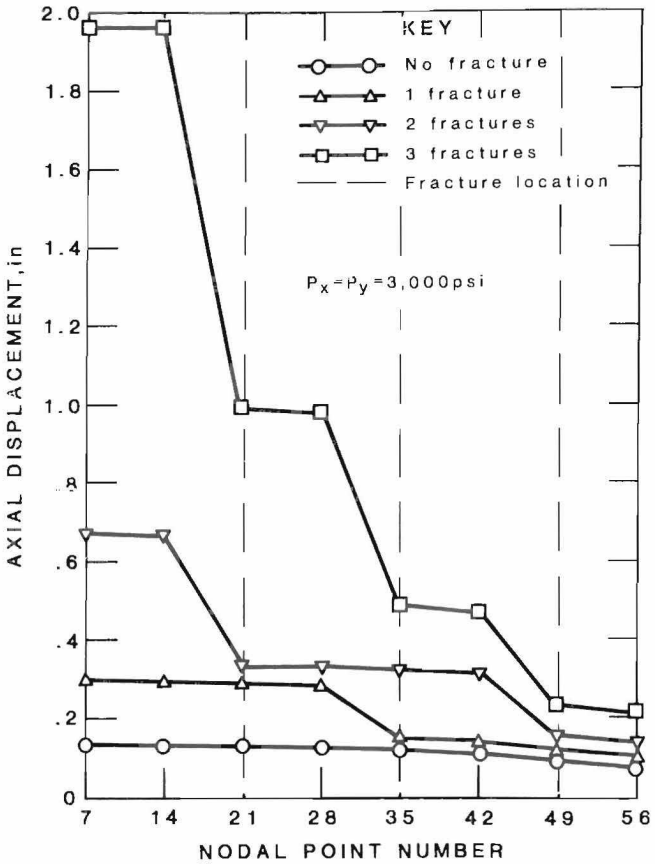

FIGURE 17. - Axial displacement along long edge of 10- by 20-ft rectangular shaft with tight fractures.

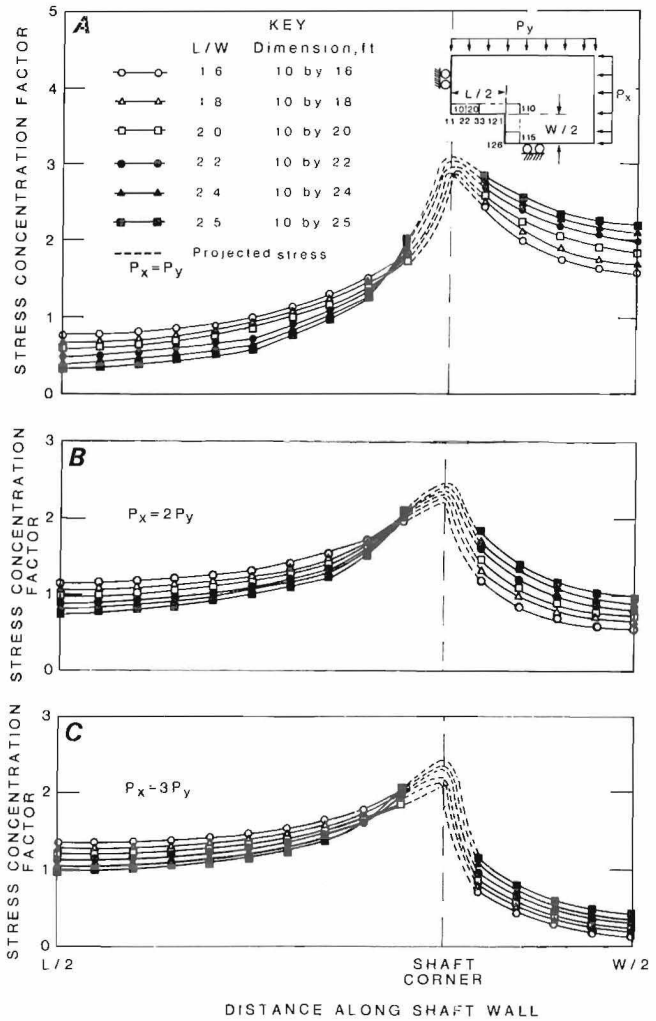

FIGURE 18. - Stress concentration as function of length-to-width ratio for rectangular shafts. *A*, 1:1 stress ratio with insert showing the model layout; *B*, 2:1 stress ratio; *C*, 3:1 stress ratio.

The effect of increasing the cross-sectional area of the shaft at a fixed L/W = 2 is shown in figure 20. With a 1:1 applied load, increasing the area by 2.4 times more than doubles the maximum displacement. A minimal effect on displacement is seen at the midpoint of the short axis. There is also an increase in the rate of change of displacement with increasing shaft cross-sectional area. Again, the significance of this parameter decreases if the preferred orientation is practiced.

Analysis was also conducted to compare relative support functions for timber, steel, and concrete, and to determine stress buildup in the support members themselves. The cross-sectional models are shown in figures 21, 22, and 23, representing timber, steel, and concrete support, respectively. Points A, B, and C represent selected locations for keying to figures 24 and 25. The rock excavation was fixed at 10 by 20 ft for the timber and steel support system and at 12 by 24 ft for the concrete liner. Obviously, the timber set will result in less usable compartment space than the steel set owing to its physical dimensions. Installation of a steel set in the concreted shaft would give the maximum

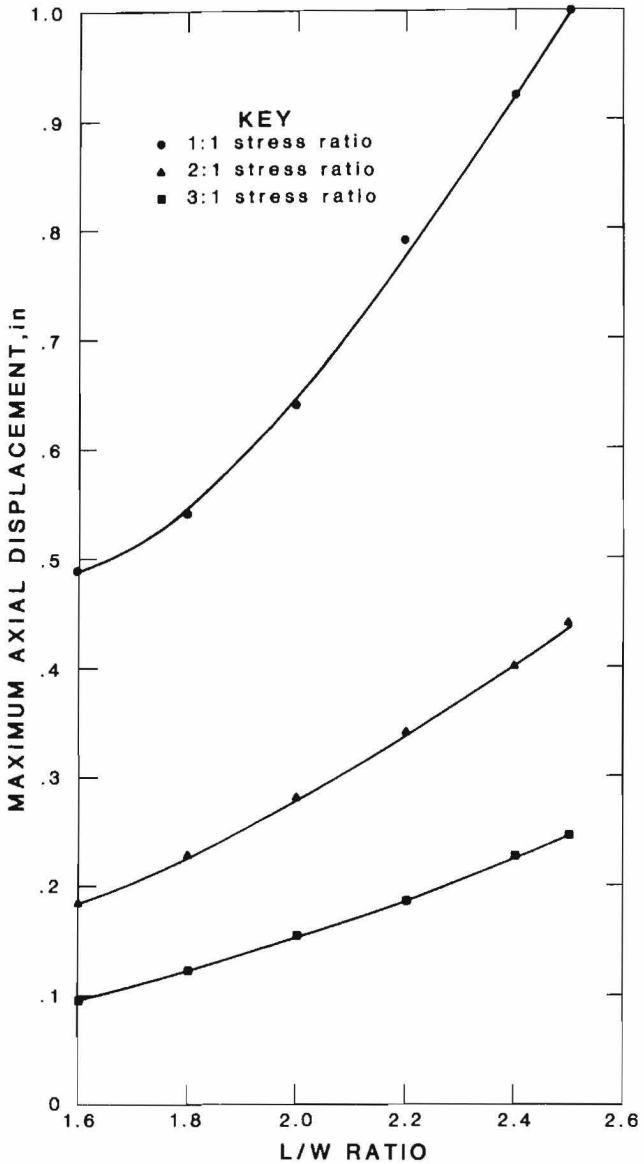

FIGURE 19. - Maximum displacement around rectangular shafts as function of length-to-width ratio for varying stress ratios.

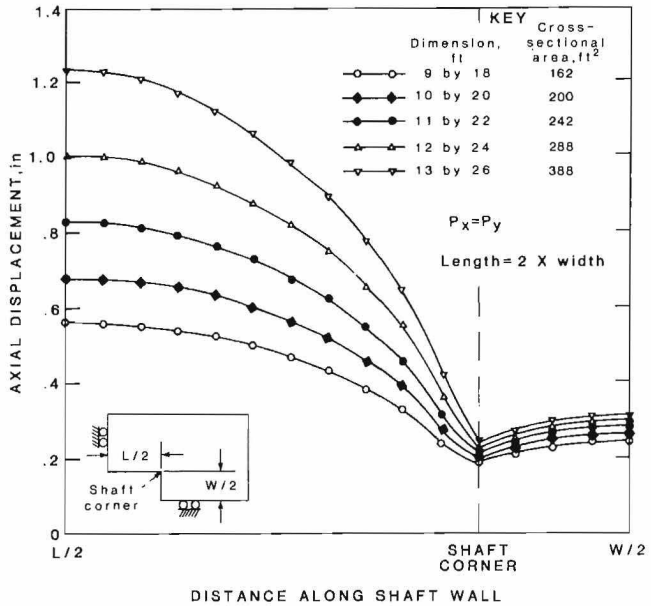

FIGURE 20. - Axial displacement around rectangular shafts as function of cross-sectional area.

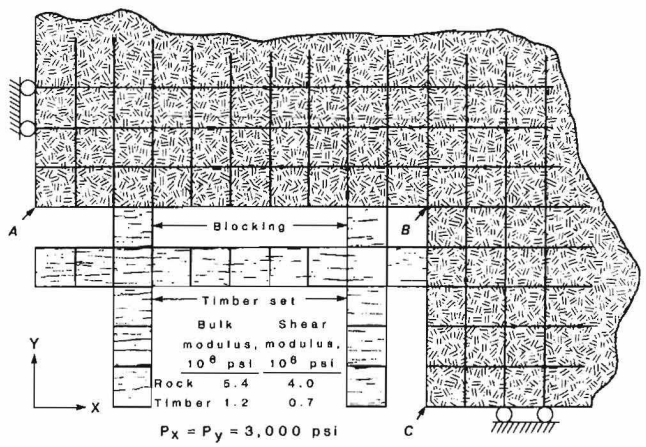

FIGURE 21. - Model for analysis of timber-supported rectangular shafts.

compartment size. A cost analysis would show the most feasible approach. For the purposes of this investigation, the inside dimension, prior to installation of the compartment structure, is the fixed parameter.

Figure 21 shows a one-quarter section of a timber-supported rectangular shaft with a three-compartment Douglas-fir set, having outside dimensions of 8 by 18 ft. The set is blocked at the corners and dividers with 12- by 12-in timber. The wall and end plates are 10 by 10 in, and the dividers are 8 by 10 in. The compressive strength of the timber is 6,000 psi when loaded parallel to the grain, and 1,000 psi perpendicular to the grain. Blocking is oriented so that load is applied perpendicular to the grain to provide for squeeze around the shaft without developing excessive load on the set.

Figure 22 shows a one-quarter section of a steel-supported shaft. Twelve-inch-square squeeze blocks are installed at the corners and end of each divider for the three-compartment set. The steel is

ASTM designation A501 hot-formed, square, carbon steel tubing, 6 by 6 in on a side with a 1-in wall thickness and a minimum yield strength of 36,000 psi.

A one-quarter section of a rectangular shaft with a 1-ft-thick concrete lining is shown in figure 23. The concrete is assumed to have a 28-day strength of 5,000 psi. Figure 24 shows the stress concentration at each element location clockwise from point *A* in figure 21, developed in the rock for each of the three types of shaft support and the unsupported case. The loading condition is uniform to isolate the effect of the support systems.

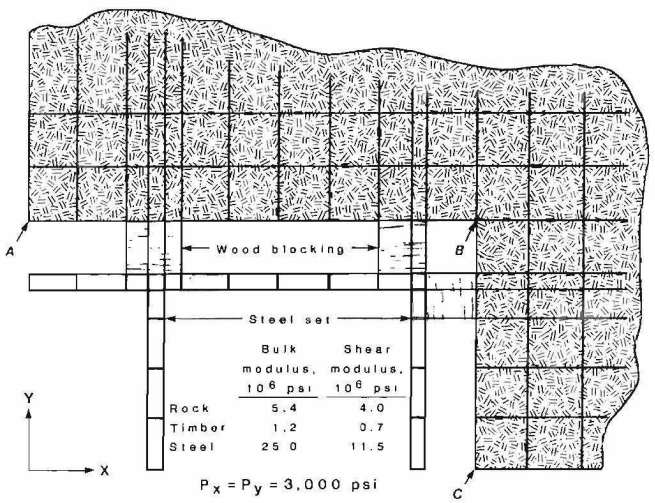

FIGURE 22. - Model for analysis of steel-supported rectangular shafts.

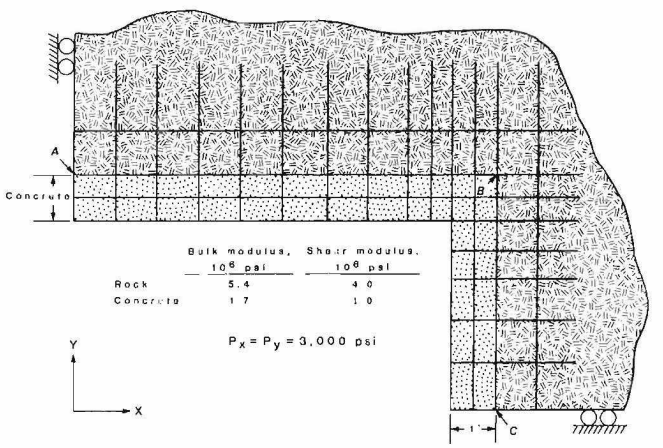

FIGURE 23. - Model for analysis of concrete-supported rectangular shafts.

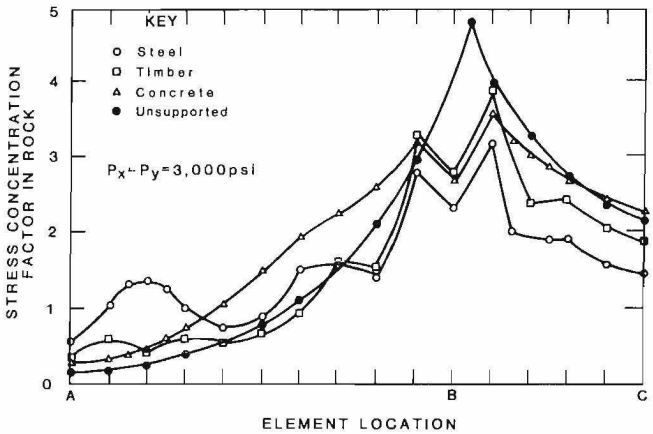

FIGURE 24. - Comparison of unsupported and steel, timber, and concrete support for 10- by 20-ft rectangular shaft in hard quartzite.

In general, there is an increase in stress concentration in the rock along the long shaft wall and a decrease along the short wall. The steel support results in local high-stress zones, particularly at blocking points. The concrete liner results in a more uniform stress distribution around the opening, although stress is actually slightly increased over the unsupported case at the midpoint of the short axis. There is also a marked decrease in shaft corner stress owing to the closely spaced blocking points. The steel set has the most dramatic effect on decreasing rock stress concentration, particularly along the short wall, whereas timber sets have almost a negligible effect.

The axial displacement in the rock around the rectangular shaft is shown in figure 25 for the steel, concrete, and timber supports. The steel is the most effective in reducing rock displacement into the shaft, particularly along the long axis. The concrete and timber support performs similarly, with concrete having the most effect in reducing displacement along the short axis.

Stress distribution in the timber, steel, and concrete is of critical importance. Figure 26 shows the maximum compressive stress in the timber for the same models and loading conditions. The largest stress occurs in the end plates

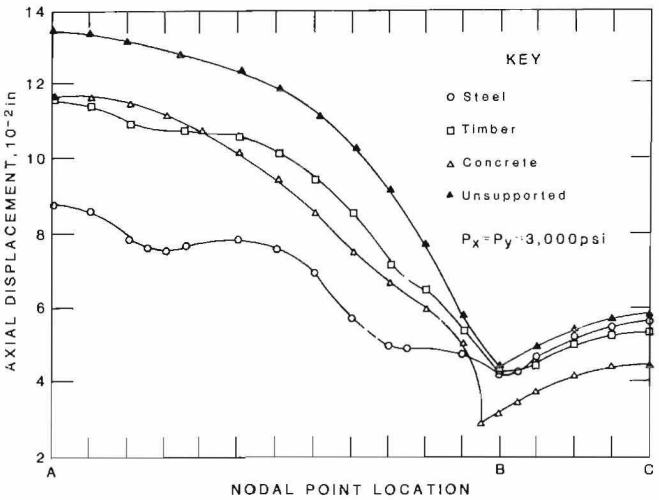

FIGURE 25. - Axial displacement in rock around 10- by 20-ft rectangular shaft in hard quartzite unsupported and supported with steel, timber, and concrete.

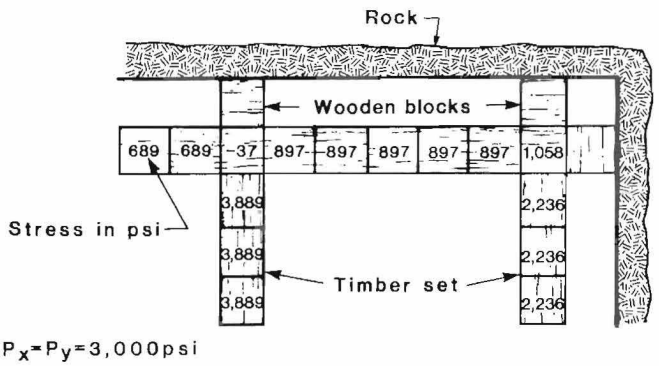

FIGURE 26. - Maximum compressive stress distribution in timber shaft set.

and dividers, being about one-third and two-thirds of the compressive strength (parallel with the grain), respectively.

For the steel-supported shaft (fig. 27), the same trend is noted. Stresses in the steel end plate and divider come very close to yield, and elastic instabilities such as buckling or twisting might become a serious problem.

Stresses in the 1-ft-thick concrete lining are shown in figure 28 for uniform and biaxial loading conditions. For uniform loading, stress is virtually zero at the midpoint of the long wall, increasing sharply to critical levels in the corner, and then down to about 50 pct of yield at the midpoint of the short axis. For the 2:1 and 3:1 loading, the stress remains

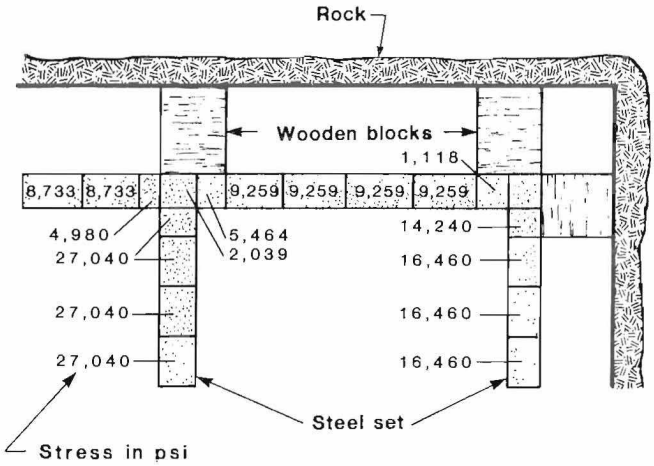

FIGURE 27. - Maximum compressive stress distribution in steel shaft set.

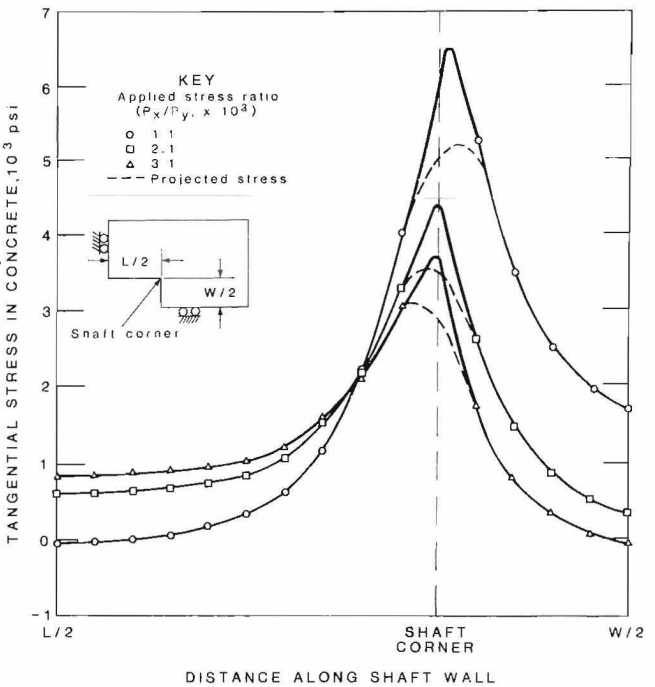

FIGURE 28. - Maximum tangential stress distribution in 1-ft-thick concrete lining.

fairly constant, except at the corners, where it again approaches the yield strength. The stress concentration in the corners is somewhat hypothetical because sharp corners are highly unlikely. A much smoother transition of stress on either side, as indicated by the dashed line, is more realistic.

ELLIPTICAL SHAFTS

An elliptical shaft has much the same design considerations as a rectangular shaft, and the correct orientation with respect to the stress field and geologic discontinuities must be maintained. The main structural advantage is that there are no sharp corners, thus eliminating critical stress concentrations. Theoretically, if the ratio between major and minor axes is the same as the ratio of applied stresses, with the major stress oriented parallel to the long axis, a uniform stress exists around the opening (fig. 29).

Thus, an elliptical shape would appear to offer the advantages of both circular and rectangular shapes from a structural standpoint. However, few elliptical shafts have been constructed owing to difficulties in excavation and support and installation of the sets and conveyances. Considering the difficulty in determining the ratio and direction of prevailing stresses, the structural advantages might lose their significance. Finite-element analysis was conducted, nevertheless, to investigate the structural aspects of this shape, particularly when a concrete lining is installed.

Figure 29 shows the stress concentration on the innermost layer of rock for a uniform loading condition with different concrete thicknesses and unsupported with a 2:1 stress ratio. The inner rock layer is represented by elements 20 through 440 for the unsupported opening, 16 through 436 with a 1-ft-thick concrete lining, and 14 through 434 with a 2-ft-thick lining. For the uniform loading condition, there is a slight increase in rock stress due to the concrete lining at the midpoint of the long radius of the shaft, with a significant decrease in stress at the midpoint of the short radius. Little advantage is gained by going from a 1- to a 2-ft lining, the benefits of increasing thickness being negated by the greater rock excavation required.

The elliptical opening with a concrete lining behaves similar to the rectangular opening (figs. 24-25). Installation of a liner slightly increases stress levels along the long wall. However, high

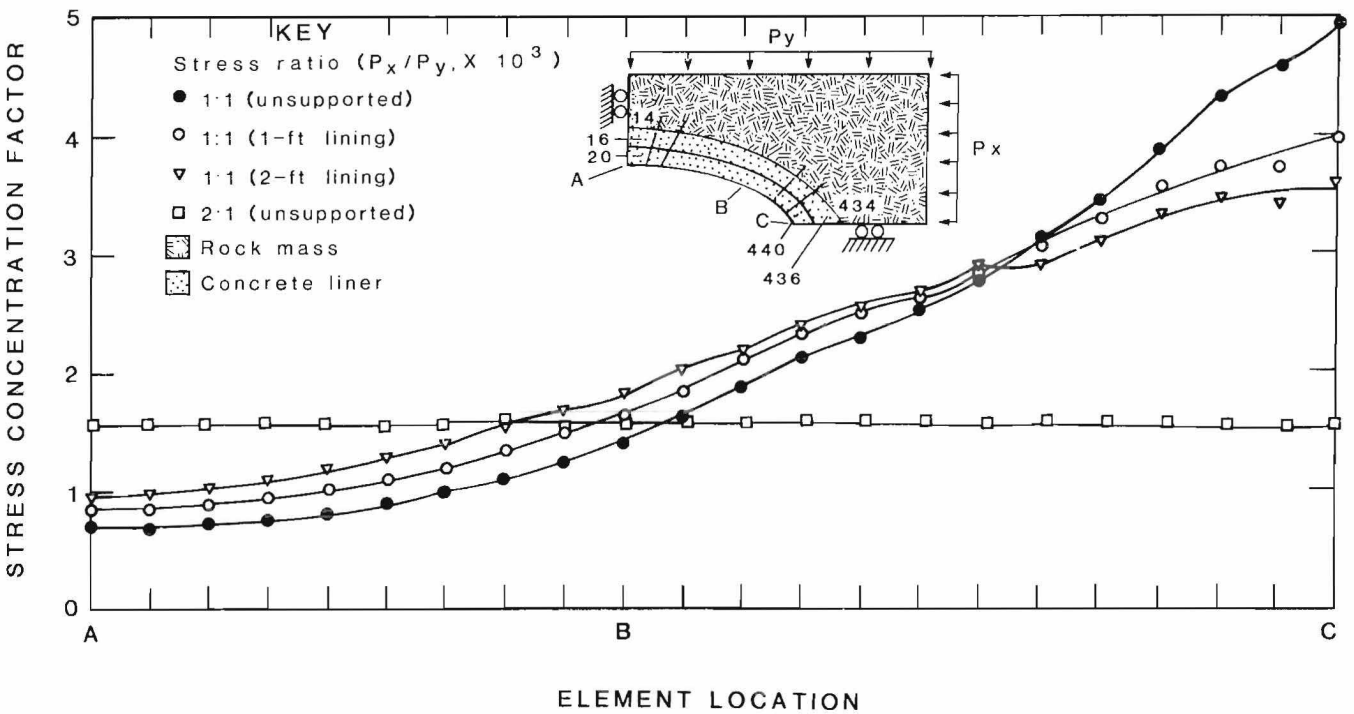

FIGURE 29. - Stress concentration in rocks around supported and unsupported 10- by 20-ft elliptical shaft for different stress ratios.

stress buildup is eliminated at the corners and decreased along the short wall. More detailed analyses of an elliptical opening are beyond the scope of this report, considering the relative usage of this configuration and its similarity to a rectangular shape.

TIME EFFECTS

Time dependency of the rock mass is also a very critical parameter from the standpoint of both design and construction. If the yield point of the rock is not exceeded and no viscoelastic behavior is mobilized, then the shaft wall rock is self-supporting and reaches equilibrium as soon as the shaft bottom advances sufficiently to eliminate end effects. However, for the depths and stress levels encountered in a deep-mine environment, the stress in the rock mass often exceeds the yield point, and time-dependent deformation, or "creep," often occurs.

Rock creep is a rather complicated deformational characteristic. Several mathematical models have been used to simulate different types of creep, as shown previously by equations 21 through 24. If the applied load and the strain rate are known, from either laboratory creep tests or in situ measurement, the coefficient of viscosity of the rock can be computed. Or, if the coefficient of viscosity is given and the applied load is assumed, the strain rate may be calculated. If time is also known, the total strain and/or deformation may be computed.

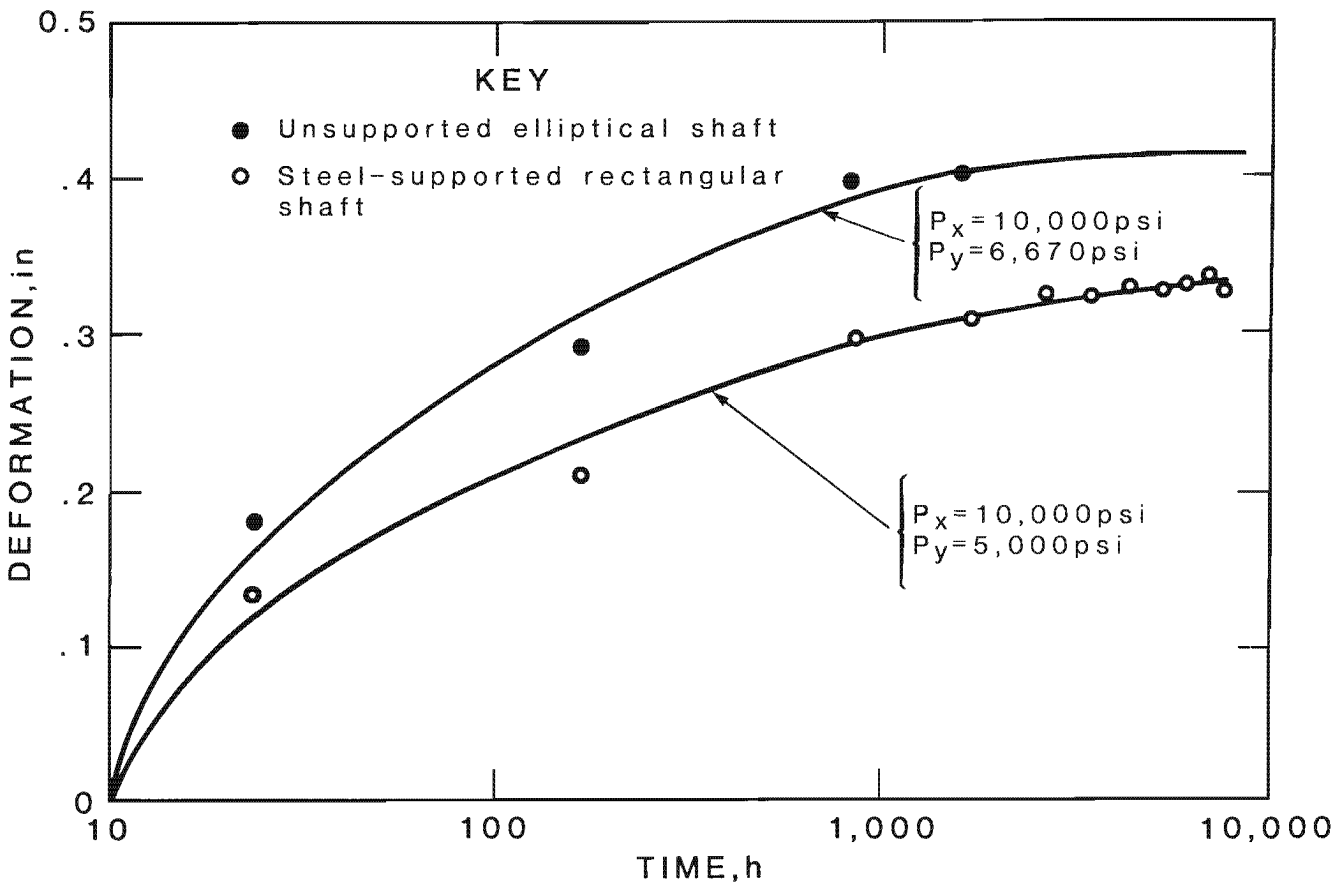

FIGURE 30. - Rock deformation versus time for 10- by 20-ft elliptical and rectangular shafts.

The viscoelastic analyses in this study used creep test results from several NX-size quartzite samples. Figure 30 illustrates the time-deformation relationship for an unsupported 10- by 20-ft elliptical shaft and a steel-supported 10- by 20-ft rectangular shaft. The radial deformation at the midpoint of the major axis of the elliptical shaft is shown. Secondary, or steady-state, creep is reached at approximately 1,000 h (6 weeks) and continues at a rate of about 4×10^{-6} in/h. Stability has still not been achieved by 10,000 h (>1 yr), and support and confinement obviously need to be provided.

The axial deformation at the midpoint of the long side of a rectangular shaft with steel support is also shown. Steady-state creep is reached in less than 1,000 h and continues at the rate of about 3×10^{-6} in/h. The load levels applied to both models are typical of what might be expected in a deep mine shaft. Although viscoelastic behavior has not been investigated in detail owing to difficulties with the finite-element code, it obviously has a major influence on shaft stability.

DISCUSSION AND CONCLUSIONS

The relative merits of different shaft designs are well known within the context of construction and service characteristics. However, little is known about the structural performance. With the finite-element technique, the structural aspects of design and construction variables have been investigated. The present study uses a two-dimensional approach.

Stress and physical property measurements from deep-vein mines provide realistic input data. Horizontal stresses are larger than vertical stress and are biaxial, ranging from a 1.25 to a 2.73 ratio. Physical property input reflects rock that is generally hard and brittle, and strength and elastic properties are highly variable, depending on mineral content, grain composition, and rock type.

Mathematical modeling using finite elements incorporates values of field and laboratory-determined stress, physical properties, and geologic data as "fixed" input. "Variable" parameters, or those that may be designed into the system, include shaft size, shape, orientation, and type and dimension of shaft support. Three primary modes of deformation, elastic, plastic,and viscoelastic, are simulated. Shaft stability is based on stress concentration and displacement for elastic solutions and yield factors for plastic analysis.

The most common shaft shape is circular, and as is well known, it is most stable with uniform loading. At deeper levels, as the rock stress approaches the yield point, plastic behavior results in better stress flow and arching, thus further favoring the circular shape. As the stress ratio becomes strongly biaxial, the stress concentration in the shaft wall, 90° from the maximum stress direction, increases significantly. Tensile loading also develops parallel with the line of maximum applied stress for this extreme loading condition.

Concrete lining may decrease the tangential stress at the concrete-rock interface by limiting deformation, depending on the ratio of applied stresses. Increasing the concrete thickness has little effect on reducing rock stress. Although not considered in this study, in actual construction the tangential rock stress and liner stress are largely dependent on distance above the shaft bottom before lining is installed, and on the time-stiffness function of the concrete. The increased excavation required and exposure of additional rock surface and planes of weakness would probably cancel any benefits obtained from increasing the thickness of the liner. Plastic analyses of circular shafts show similar results, with yield zones occurring at the maximum stress concentrations found from elastic solution.

Rectangular shafts are extensively analyzed for various combinations of orientation, applied load, geologic discontinuities, shaft size, and support systems. The most important design decision for a rectangular shaft is its orientation, with respect to both the in situ stress field and the geologic weakness planes. The most unfavorable orientation is with the long axis of the shaft oriented normal to the major stress in a biaxial stress field. Conversely, the best orientation is with the major stress and long shaft axis parallel, resulting in minimal yielding in the rock. If the stress field is highly unidirectional, such as near a fault or mining area, yielding may occur regardless of orientation. Likewise, if the stress field is uniform, orientation is irrelevant and general yielding is evident.

Bedding planes, joint systems, type and size of the support system, and shaft size affect structural performance. A cursory examination of interbedding and jointing shows that geologic defects have the most significant effect on stress concentration and displacement. In fact, consideration of the anisotropy of the medium might be the controlling design consideration. For example, an interbedded quartzite-argillite medium shows significant stress concentration at the midpoint of the short axis. Interbedding also significantly increases the displacement profile of the shaft wall. For uniform loading, displacement is increased several times over that with the nonbedded condition, regardless of orientation.

Displacement is also dependent on the degree of joints and fracture systems in the rock mass, subject to frictional resistance between the joint surfaces and frequency. Joints with negligible shear resistance result in displacement at the midpoint of the long axis that is many times that of the unfractured medium.

The L/W ratio of the axes for rectangular shafts also has varying degrees of influence on stresses and displacements that may be encountered. The effect of L/W on the stress concentration is negligible, particularly if the preferred orientation with respect to stress ratio is practiced. The axial displacement, however, is changed significantly at the midpoint of the long shaft axis, being nearly doubled by increasing the L/W by 60 pct. Shaft size also affects displacement; by increasing shaft cross-sectional area by 2.4 times at an L/W of 2:1 and a 1:1 load ratio, displacement at the long axis midpoint is more than doubled.

Timber-, steel-, and concrete-supported rectangular shafts show little difference in support function, compared to the unsupported case. The concrete lining results in a smoother stress distribution around the opening, whereas the steel support causes some local high stress concentrations. The steel support system is most effective in reducing axial displacement and stress concentration. However, dividers and end plates of both the steel and timber systems might become critically stressed when subjected to even nominal in situ stress. This is also evident in the corners for a concrete-lined opening.

Elliptical openings are subject to much the same design consideration as rectangular openings. The preferred orientation is with the long axis oriented parallel with the major stress direction. The principal advantage of this shape is elimination of "critical" stresses developed in the corners of rectangular shafts. If the ratio between major and minor axes is the same as the applied stress ratio, the stress concentration is uniform.

Time effects become of increasing importance, as depths currently being mined result in the yield point of the rock being exceeded. Viscoelastic or time-dependent properties are definitely a factor in deciding long-term shaft stability, and increasing emphasis is being placed on determining these properties.

In summary, the many structural aspects involved with the design of deep underground shafts are complex and difficult to evaluate. This report obviously does not cover every possible combination of applied load, orientation, geologic defects, rock mass behavioral modes, opening dimensions, or support concepts. It

has been shown that the magnitude, direction, and ratio of applied stress and rock mass anisotropy are keys to determining shaft stability. Little can be done to alter the magnitude and direction of the prevailing stress field around the shaft opening. Likewise, geologic discontinuities are impossible to eliminate, although their strength properties may be altered by crossbolting, grouting, and dewatering. However, these parameters can be determined before construction begins, so that the structural characteristics of the shaft and support can be optimized.

A realistic conceptual framework has been developed upon which to examine the rock and support interaction in deep mine shafts. Structural analysis techniques can overcome some of the historical difficulties with shaft design by defining the field data requirements and structural sensitivity of various design and construction parameters.

BIBLIOGRAPHY

1. Abel, J. F., Jr., J. E. Davis, and D. P. Richards. Concrete Shaft Lining Design. Paper in Proceedings 20th U.S. Sumposium on Rock Mechanics, Univ. TX, 1979, pp. 627-640.

2. Allen, M. D., S. S. M. Chan, and M. J. Beus. Correlation of In Situ Stress Measurement and Geologic Mapping in the Lucky Friday Mine, Mullan, ID. Paper in Proceedings 16th Annual Symposium on Engineering Geology and Soils Engineering, ID Trans. Dep., 1978, pp. 1-22.

3. Beus, M. J., and S. S. M. Chan. Preliminary Structural Design for Deep Shafts in the Coeur d'Alene District, Idaho. Pres. at AIME Annu. Meeting, Las Vegas, NV, Feb. 22-26, 1976. Soc. Min. Eng. AIME preprint 76-AM-15, 24 pp.

4. _____. Shaft Design in the Coeur d'Alene Mining District, Idaho - Results of In Situ Stress and Physical Property Measurements. BuMines RI 8435, 1980, 39 pp.

5. Beus, M. J., E. L. Phillips, and G. G. Waddell. Instrument To Measure the Initial Deformation of Rock Around Underground Openings. BuMines RI 8275, 1978, 40 pp.

6. Bucky, P. B. Fundamental Considerations in Block Caving. Q. CO Sch. Mines, v. 51, No. 3, 1956, pp. 127-143.

7. Chan, S. S. M. A Case Study of In Situ Rock Deformation Behavior for the Design of Ground Support System. BuMines OFR 44-73, 1972, 130 pp.; NTIS PB 221 880/AS.

8. Chan, S. S. M, and M. J. Beus. Ground Stress Determination in the Coeur d'Alene District Using the CSIR Technique. Paper in Proceedings, Pacific Northwest Metals and Minerals Conference. AIME, 1976, pp. 1-16.

9. _____. Interpretation of In Situ Deformational Behavior of a Rectangular Test Shaft Using Finite-Element Method. Paper in Field Measurements in Rock Mechanics, ed. by K. Kovari. A. S. Balkema, Rotterdam, v. 2, 1977, pp. 889-903.

10. Coates, D. F. Shafts, Drifts, and Tunnels. Ch. 3 in Rock Mechanics Principles. Can. Dep. Energy, Mines and Resour., Mines Branch Monog. 874, 1970, pp. 3-1 to 3-42.

11. Coates, D. F., and Y. S. Yu. Three-Dimensional Stress Distributions Around a Cylindrical Hole and Anchor. Paper in Proceedings 2d Congress, International Society of Rock Mechanics. ISRM, v. 3, 1970, pp. 175-180.

12. Cornish, E. Vertical Shafts. CO Sch. Mines Miner. Ind. Bull., v. 10, No. 5, Sept. 1967, 23 pp.

13. Dar, S. M., and R. C. Bates. Stress Analysis of Hollow Cylindrical Inclusions. J. Geotech. Eng. Div., ASCE, v. 100, Feb. 1974, pp. 123-138.

14. _____. Analysis of Backpacked Liners. J. Geotech. Eng. Div., ASCE, v. 102, July 1976, pp. 739-759.

15. Dravo Corp. Analysis of Large-Scale Noncoal Underground Mining Methods. (contract S0122059). BuMines OFR 36-74, 1974, pp. 176-268; NTIS PB 234 555/AS.

16. Durelli, A. J. Applied Stress Analysis. Prentice-Hall, 1967, 180 pp.

17. Duvall, W. I. General Principles of Underground Opening Design in Competent Rock. Paper in Site Characterization, ed. by W. S. Brown, S. J. Green, and W. A. Hustrulid. Univ. UT, Salt Lake City, UT, 1976, pp. 3A1-1 to 3A1-11.

18. Ewing, R. D., and E. M. Raney. User's Guide for a Computer Program for Analytical Modeling of Rock Structure Interaction. BuMines contract H0262020, Final Rep., 1976, 95 pp.; NTIS, AD 761648-AD 761650.

19. Galanka, J. Problems of Shaft Sinking in Poland. Paper in Proceedings, Symposium on Shaft Sinking and Tunneling. Inst. Min. Eng., London, 1960, pp. 369-380.

20. Galle, E. M., and J. C. Wilhoit, Jr. Stresses Around a Wellbore due to Internal Pressure and Nonsymmetrical Geostatic Stress. Soc. Petrol. Eng. J., v. 2, No. 2, pp. 145-155.

21. Gnirk, P. F., and R. E. Johnson. The Deformational Behavior of a Circular Mine Shaft Situated in a Viscoelastic Medium Under Hydrostatic Stress. Paper in Proceedings, 6th Symposium on Rock Mechanics. Univ. MO, Rolla, MO, 1964, pp. 231-258.

22. Gooch, A. E., and J. P. Conway. Field Measurements and Corresponding Finite-Element Analysis of Closure During Shaft Sinking at the Lucky Friday Mine. BuMines RI 8193, 1976, 19 pp.

23. Hast, N. The State of Stress in the Upper Part of the Earth's Crust. Eng. Geol., v. 2, No. 1, 1967, pp. 5-17.

24. Herget, G., A. Pahl, and P. Oliver. Ground Stresses Below 3,000 Feet. Paper in Proceedings, 10th Canadian Rock Mechanics Symposium. Queen's Univ., Kingston, Ontario, v. 1, 1975, pp. 281-307.

25. Hetinyi, M. Handbook of Experimental Stress Analysis. Wiley, 1966, pp. 407-415.

26. Heuze, F. E., and T. G. Barbour. Analysis of Circular-Shafts in Sedimentary Rocks. Pres. at Soc. Min. Eng. AIME Fall Meeting, Tucson, AZ, Oct. 17-19, 1979. Soc. Min. Eng. AIME preprint 79-316, 4 pp.

27. Hobbs, S. W., A. B. Griggs, R. E. Wallace, and A. B. Campbell. Geology of the Coeur d'Alene District, Shoshone County, Idaho. U.S. Geol. Surv. Prof. Paper 478, 1965, 139 pp.

28. Hustrulid, W. A. Development of a Borehole Device To Determine the Modulus of Rigidity of Coal Measure Rocks. BuMines OFR 12-72, 1971, 119 pp.; NTIS PB 209 548/AS.

29. Hynd, J. G. S., and E. Singer. Some Aspects of Circular Concrete-Lined Shaft Sinking. Paper in Proceedings Pacific Northwest Metals and Minerals Conference. AIME, 1973, pp. 1-22.

30. Karwoski, W. J. Deep Shaft Design Parameters. Paper in Proceedings Pacific Northwest Metals and Minerals Conference. AIME, 1973, pp. 22-52.

31. Karwoski, W. J., and D. E. Van Dillen. Applications of BMINES Three-Dimensional Finite-Element Computer Code to Large Mine Structural Problems. Paper in Proceedings 19th U.S. Symposium on Rock Mechanics. Univ. NV, Stateline, NV, v. 2, 1978, pp. 114-120.

32. Leeman, E. R. The Measurement of Stress in Rock. J. S. Afr. Inst. Min. and Metall., v. 65, 1967, pp. 45-144, 254-284.

33. _____. The "Doorstopper" and Triaxial Rock Stress Measuring Instrument Developed by the CSIR. J. S. Afr. Inst. Min. and Metall., v. 69, 1969, pp. 305-339.

34. Linder, E. N., and J. A. Halpern. In Situ Stress and Analysis. Paper in Proceedings 18th U.S. Symposium on Rock Mechanics. CO Sch. Mines, Keystone, CO, 1977, pp. 4C1-1 to 4C1-7.

35. McWilliams, J. R., and E. G. Erickson. Methods and Costs of Shaft Sinking in the Coeur d'Alene District, Shoshone County, Idaho. BuMines IC 7961, 1960, 49 pp.

36. Morrison, R. G. K. A Philosophy of Ground Control. Ontario Dep. Mines, Toronto, Ontario, Canada, 1976, 182 pp.

37. Nichols, T. G., Jr., J. F. Abel, Jr., and F. T. Lee. A Solid-Inclusion Borehole Probe To Determine Three-Dimensional Stress Changes at a Point in a Rock Mass. U.S. Geol. Surv. Bull 1258-C, 1968, pp. C1-C28.

38. Obert, L., and W. I. Duvall. Rock Mechanics and the Design of Structures in Rock. Wiley, 1967, 360 pp.

39. Obert, L., W. I. Duvall, and R. H. Merrill. Design of Underground Openings in Competent Rock. BuMines B. 587, 1960, 36 pp.

40. Obert, L., and D. E. Stephenson. Stress Conditions Under Which Core Discing Occurs. Trans. AIME, v. 232, 1965, pp. 227-234.

41. Ostrowski, W. J. S. Design Considerations for Modern Shaft Linings. Can. Min. and Metall. Bull., Oct. 1972, pp. 58-72.

42. Pariseau, W. G. Estimation of Support Load Requirements for Underground Mining Openings by Computer Simulation of the Mining Sequence. Pres. at Soc. Min. Eng. AIME Fall Meeting, Salt Lake City, UT, Sept. 10-12, 1975. Soc. Min. Eng. AIME preprint 75-AM-358, 36 pp.

43. Patricio, J. G., and M. J. Beus. Determination of In Situ Modulus of Deformation in Hard Rock Mines of the Coeur d'Alene District, Idaho. Paper in Proceedings, 17th U.S. Symposium on Rock Mechanics. Univ. UT, Salt Lake City, UT, 1976, pp. 4B9-1 to 4B9-7.

44. Peck, R. B. Shafts and Shaft Linings. Ch. 6--Some Design Considerations in the Selection of Underground Support Systems. DOT Contract 3-0152, 1969, pp. 78-105; NTIS PB 190443.

45. Procter, R. V., and T. L. White. Rock Tunneling With Steel Supports. Commercial Shearing and Stamping Co., Youngstown, OH, 1946, 282 pp.

46. Raleigh, C. B. Crustal Stress and Global Tectonics. Paper in Proceedings 3d International Symposium on Rock Mech. Natl. Acad. Sci., 1974, pp. 593-597.

47. Ranken, R. E., and J. G. Ghaboussi. Tunnel Design Considerations: Analysis of Stresses and Deformation Around Advancing Tunnels. Univ. IL, Rep. FRA OR&D 75-84, DOT Rep. UILU-Eng 75-2016, Aug. 1975, 250 pp.

48. Richards, D. P., and J. F. Abel, Jr. Shaft Lining Design in Rock. Pres. at 108th AIME Annu. Mtg. New Orleans, LA, Feb. 22, 1979. Soc. Min. Eng. AIME preprint ____, 7 pp.

49. Roberts, A. Geotechnology, An Introductory Text for Students and Engineers. Pergamon, 1977, 347 pp.

50. Schlage, R. Development of Large Diameter Drilling Equipment (Phase II), Vols. III, IV, and V. Shaft Liner Systems (DOE contract DE-AC22-76ET12482, Fenix & Scisson, Inc.). Final Rep., Sept. 1981.

51. Seely, F. B., and J. D. Smith. Advanced Mechanics of Materials. Wiley, 2d ed., 1952, pp. 295-319.

52. Swaisgood, J. R., and R. E. Versaw. Geotechnical Investigations for Mine Shafts. Paper in Proceedings Pacific Northwest Metals and Minerals Conference AIME, 1973, pp. 52-70.

53. Timoshenko, S. P., and J. N. Goodier. Theory of Elasticity. McGraw-Hill, 3d ed., 1970, pp. 68-71, 80-96.

54. Trollope, D. H. The Stability of Deep Circular Shafts in Hard Rock. Paper in Proceedings 2d Congress, International Society of Rock Mechanics, ISRM, v. 2, 1970, pp. 669-673.

55. U.S. Army Corps of Engineers. Engineering and Design - Tunnels and Shafts in Rock, Pt. 2. Corps of Engineers Draft Man. EM 1110-2-2901, Dec. 1973, 149 pp.

56. Van Dillan, D. E., R. W. Fellner, and R. D. Ewing. Modernization of the BMINES Computer Code - Volume 1: User's Guide. (contract H0282022 Agbabian Assoc.). OT-1-83, 1981, 614 pp.; NTIS PB 83-221564.

57. Vutukuri, V. S., R. D. Lama, and S. S. Saluja. Handbook on Mechanical Properties of Rocks--Testing Techniques and Results. Trans Tech Publications, Bay Village, OH, v. 1, 1974, 280 pp.

58. Wilson, J. W. The Protection of Vertical Shafts in Deep Level, Hard-Rock Mines. Paper in Proceedings 17th U.S. Symposium on Rock Mechanics. Univ. UT, Snowbird, UT, 1976, pp. 3A5-1 to 3A5-12.

59. Zahary, G., and K. Unrug. Reinforced Concrete as a Shaft Lining. Paper in Proceedings 8th Canadian Rock Mechanics Symposium. Can. Dep. Energy, Mines and Resour., Mines Branch, Ottawa, Canada, 1973, pp. 265-282.

☆U.S GPO: 1985-505-019/20,088

INT.-BU.OF MINES,PGH.,PA. 28077